NTNU
Norwegian University of
Science and Technology

Reduction Mechanisms in Manganese Ore and Deposition of Carbon from Natural Gas

Stine Svoen

Materials Science and Engineering
Submission date: June 2017
Supervisor: Leiv Kolbeinsen, IMA
Co-supervisor: Eli Ringdalen, SINTEF

Norwegian University of Science and Technology
Department of Materials Science and Engineering

Reduction Mechanisms in Manganese Ore and Deposition of Carbon from Natural Gas

Stine Marie Wagner Svoen

Supervisor Professor Leiv Kolbeinsen

Co-supervisor Dr. Eli Ringdalen

Department of Material Science and Engineering

Norwegian University of Science and Technology, NTNU

NTNU

Kunnskap for en bedre verden

1 Abstract

This report investigates the deposition of carbon from natural gas onto manganese ore and the effect of reduction of the higher manganese oxides. Manganese ore has been heated in an argon atmosphere, before methane was purged through the ore. To distinguish the reduction caused by heat and methane, experiments where manganese oxide was only heated in argon was executed. The most interesting samples were further studied in an electron probe microscope.

The contemporary deposition of carbon and reduction is discussed, and compared with results from the project completed in the course TMT4500 Material Technology Specialization Project.

2 Sammendrag

Deponering av karbon fra naturgass på mangan malm og effekten av reduksjon har blitt undersøkt. Dette har blitt gjort ved at manganmalm har blitt varmet opp i en argon atmosfære, før den har blitt holdt på en konstant temperatur mens metan gass har blitt blåst igjennom. For å skille reduksjon som følge av varme og metangassen, har forsøk blitt gjort der malm utelukkende ble varmet opp i argon. De mest interessante prøvene har deretter blitt studert i mikrosonde.

Den samtidige deponeringen av karbon og redusering av de høyere manganoksidene har blitt diskutert, og sammenlignet med resultatene fra rapporten som ble skrevet i forbindelse med kurset TMT4500 Materials Technology Specialization Project.

3 Preface

I would like to thank my supervisors, Professor Leiv Kolbeinsen and Dr. Eli Ringdalen, for invaluable help on the thesis. Further have Pål Tetlie, Ingeborg Solheim, Jonas Einan Gjøvik and Bendik Sægrov been crucial for the furnace set-up. Xiang Li has also given helpful inputs.

At last, I am very grateful to ERAMET Norway, SINTEF, as well as FFF and research council for funding the project.

Contents

1 Introduction

1.1 Manganese

Manganese is the second most common transition metal in the earth's crust, second only to iron. It does not occur naturally in its metallic form, and is most often found as oxides, carbonates and silicates. Iron and manganese are neighbors in the periodic table, and are usually found together in their oxidized state [1].

In its metallic form, manganese is a stronger metal than iron, but due to its brittle nature, its usage is limited alone. Practically the entire amount of produced manganese is used as an alloying metal in steel, but it's also used as an alloying element in cast iron, aluminum, magnesium and copper alloys. The primary non-ferrous application of manganese is as an alloying element in aluminum, where it increases the corrosion resistance [2]. Pure manganese has its melting point at 1244^{o} C and atomic mass equal to 54.938 [3].

Figure 1: Manganese in its metallic form [4]

1.2 Production of manganese ferroalloys

There are two main routes for commercially production of manganese ferroalloys, either in a blast furnace where coke is used as the main energy source and reduction agent, or in a submerged arc furnace, where electricity is used to heat the charge, and coke operates as an electric resistance and a reducing agent.

The submerged arc furnace is most common production route today, as it has several advantages over the blast furnace; higher yield of manganese from the ore, less consumption of carbon, lower quality reducing agents, ability to produce different grades of alloys as well as the ability to produce both HC FeMn and SiMn.

In general, the furnace has a circular shape and three graphite electrodes, each connected to a separate, electric phase. Electricity will run through the electrodes to the underside, where the electrode is in contact with the coke in the base of furnace.

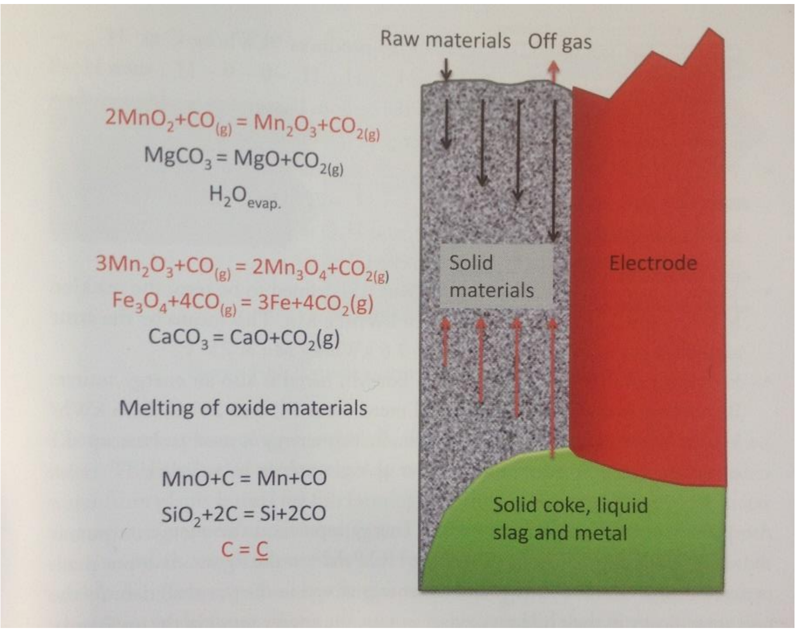

Figure 2: Schematic view of a manganese furnace [5]

Three different zones are found inside the submerged arc furnace, *pre-reduction zone*, c*oke bed zone* and *metal layer*. The metal layer doesn't affect the reduction process inside the furnace, and is therefore disregarded here. The charge enters the pre-reduction zone in the furnace at 25^{o}C, and it is here the higher manganese oxides (MnO_2, Mn_2O_3, Mn_3O_4) are reduced to lower manganese oxides. These reduction processes are exothermic, and the energy released will contribute to heat the charge entering the furnace.

As the charge ascend in the furnace, the temperature will increase, and when the ore and fluxes start to melt, it has arrived in the coke bed zone. The coke will remain solid here, while the liquefied flux and ore will form an oxide mix, also known as slag, and metallic manganese. The metal will descend to the bottom of the furnace, with the slag floating on top.

1.3 Natural gas and substitution of coke

Because of the recent years' attention to the environmental pollution issues, the Norwegian metal industry is striving to find processes making the production of metal more environmental friendly. The substitution of coke with carbon from natural gas has the potential to reduce CO_2 emissions by 4-15 ton per ton of coke substituted. This calculation is done by Xiang Li.

Coal is a critical raw material, and a substitution of coke with natural gas would decrease the demand of coke production. A worldwide trend of decreasing quality in petroleum coke [6] cause the emerge of the need of a cleaner carbon source and in general, gas contains less trace elements with the exception of sulphur, furthermore making it more interesting to investigate the possibility of substituting coke with carbon from natural gas. Natural gas is also the worlds' largest source of fossil fuel [7].

In the coking process, where coke is made from coal through heating, the removal of sulphur and phosphorus is possible [1]. Impurities of sulphur and phosphorus are detrimental to the mechanical properties of steel, and therefore unwanted in the finished manganese product. While sulphur's oxide potential allows it to be removed from the metal by slag refining in a desulphurization process [8], this is not possible for phosphorus because of its low oxide stability.

Depending of the source, natural gas consists for the largest part of methane, making up 85-95% of the whole [7]. Light alkanes ($C \leq 6$) and smaller amounts of CO_2 and nitrogen make up the rest. If there is a larger amount of higher order hydrocarbons in the gas i.e. hydrocarbons with longer chains, a lower H:C ratio will be present in the gas, which can have an impact on the decomposition or the *cracking* of methane [9].

1.4 Scope of project

The project investigates the possibility of depositing carbon from natural gas onto manganese ore at temperatures between 700ºC and 1100ºC. Earlier experiments in the course TMT4500 Material Technology Specialization Project [10] proved it possible to deposit carbon onto the surface of manganese ore. The higher manganese oxides are easily reduced and may influence the deposition of carbon.

This report explores the mechanisms for deposition of carbon from natural gas, and the contemporary deposition of carbon and reduction of the higher manganese oxides.

It will further be investigated what reductions are due to the heating process, and what is caused by methane gas.

2 Theory

2.1 Methane

2.1.1 Cracking

Methane will decompose, or *crack*, into carbon black and hydrogen gas, following reaction (1), when the temperatures reaches 547.6ºC, according to calculations using data from HSC 7.18Z and assuming thermodynamic equilibrium. All further calculations and enthalpy data also originates from HSC 7.18Z.

$$CH_4(g) \rightarrow C(s) + 2H_2\,(g) \qquad \Delta H^o_{1273} = 90.3\ \frac{kJ}{mol}\,(1)$$

Cracking of methane is an endothermic reaction, and hence needs energy from the surroundings to proceed. As earlier mentioned, equilibrium calculations state that reaction (1) will proceed when the temperature reaches 547.6ºC, but due to the reaction kinetics, the temperature needs to be higher. A purely thermal cracking of methane needs temperatures at approximately 1200ºC, due to strong C-H bonds [11].

Catalysts such as copper and iron can lower the temperature at which decomposition takes place. The effectiveness of the catalyst depends on the carbon and diffusion phenomena – this cause a reduction in the active surface area of the catalyst, making it inefficient as a catalyst to reduce the natural gas [12]. When catalysts are utilized to crack methane, the reduction process can take place at temperatures as low as 500ºC [13].

2.1.2 Methane as a reducing agent

Methane can work as a reducing agent, where it will reduce the oxide in question. This is done at temperatures where methane is metastable, above 550ºC at standard conditions [14]. The activity of graphitic carbon is 1 here, but under these circumstances, carbon in methane will be higher, consequently having a higher reduction potential than graphitic carbon. The higher carbon activity when methane is metastable allows reductions to take place at temperatures considerably lower than those predicted by equilibrium calculations. The activity of carbon in methane relative to the activity of carbon in graphitic form is given by equation (I) [15];

$$\frac{a_{C*}}{a_{C_{GR}}} = \frac{p_{CH_4}/p_{H_2^2}}{\left(p_{CH_4}/p_{H_2^2}\right)_{GR}} \text{ (I)}$$

Here a_{C*} is the activity of carbon in metastable methane gas, $a_{C_{GR}}$ the activity of carbon in graphite, p_{CH_4} is the partial pressure of methane and $p_{H_2^2}$ is the partial pressure of hydrogen.

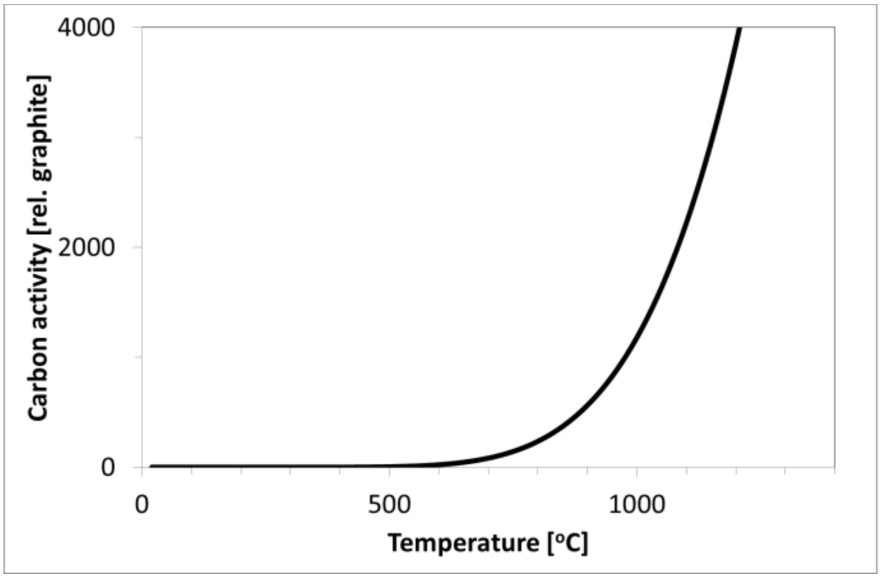

Figure 3: Carbon activity plotted against temperature for a gas with 10% CH_4-10% H_2-80% Ar. The equilibrium ratio is plotted using FactSage, taken from Dalaker and Tetlie [15].

The progress of the reduction reaction is determined by the interactions of the methane and the oxide to be reduced. If the reaction progress is dominated by deposition of carbon, no reduction of the oxide will take place.

As methane has a great reduction potential, it can be used to produce *synthesis* gas; a gas consisting of hydrogen, carbon monoxide and usually some carbon dioxide, over a metal oxide. Given standard conditions, the temperature needed for a *methanothermal* reduction compared to that of a *carbothermal* reduction, a reduction with solid carbon, will be considerably lower. This is because the gas-solid reduction reaction with methane has a higher kinetic rate, i.e. takes place at faster pace, than that of the solid-solid reduction with carbon [16].

2.1.3 Formation of manganese carbide

The carbothermal reduction of manganese oxides, i.e. reduction with a solid carbon source, to manganese carbide commence when the temperature reaches 1340°C, following reaction (2).

$$7\ MnO + 10\ C\ (s) = Mn_7C_3 + 7\ CO\ (g) \qquad \Delta H^0_{1273} = 1775.8\frac{kJ}{mol}\ (2)$$

A methanothermal reduction of manganese oxide, where methane is used as reduction agent, will commence when T > 928°C at standard conditions [17] [18].

$$7MnO + 10\ CH_4(g) = Mn_7C_3 + 7\ CO(g) + 20\ H_2(g)\ (X) \qquad \Delta H^0_{1273} = 2678.7\frac{kJ}{mol}\ (3)$$

The formation of manganese carbide and the deposition of solid carbon depends on where the ore properties, as behavior of the ore is defined by its chemistry, mineralogy and concentration of elements [19]. The deposition of carbon is detrimental to the reduction process, as solid carbon will block the access to the core of the manganese oxide, and brings the carbon activity down to 1 [14]. According to *Olsen* [1], formation of Mn_7C_3 needs lower oxygen potential than what is attainable in the presence of CO gas at 1 atm.

Ostrovski and Zhang [14] found that manganese carbide samples quickly swelled and decrepitated in air. The rapid decomposition thus makes it hard to prepare samples for metallographic analyzes, but an addition of at least 5 % iron can stabilize the carbide.

2.1.4 Deposition of carbon

The rate of deposition of solid carbon onto a metal oxide surface with a methane containing gas is affected by the composition of the gas (ratio of methane to hydrogen), temperature and the surface area of the oxide. Catalysts are also strongly affecting the deposition of solid carbon [18].

2.2 Boudouard reaction

The Boudouard reaction is a well-known gas-solid reaction, which describes the equilibrium between solid carbon, CO and CO_2 in. The reaction proceeds as seen in (4) below.

$$2\,CO\,(g) = C\,(s) + CO_2\,(g) \qquad \Delta H^o_{298} = -172.1\frac{kJ}{mol}\ (4)$$

The reaction, shifted to the right (i.e. producing CO_2 (g) and solid carbon) is exothermic for all temperatures [20]. The Boudouard reaction is unfavorable inside the smelting furnace, as CO gas is consumed, instead of being used to reduce manganese oxides A high reaction rate is thus undesirable. The reaction rate is determined by the temperature, reactivity of the coke and the partial pressures of CO (g) and CO_2 (g), plotted in figure 4. CO_2 (g) is favored on the left-hand side of the cross section, CO (g) on the right.

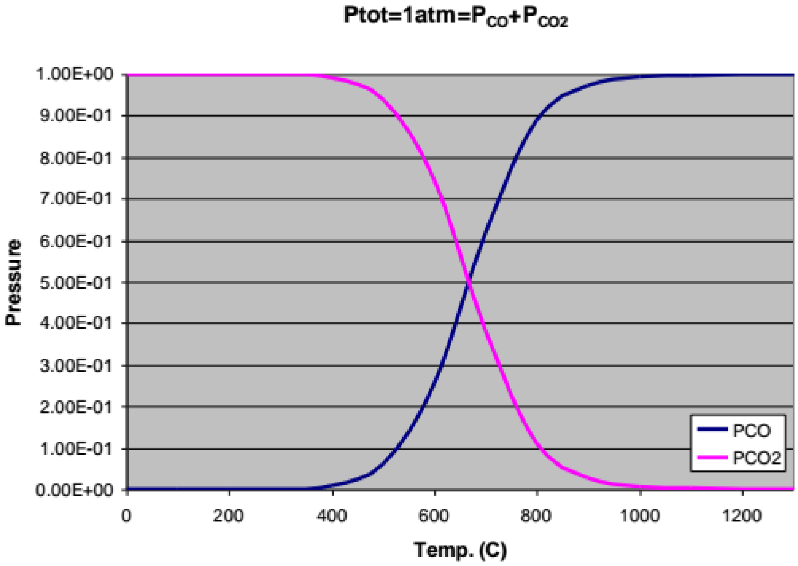

Figure 4: Equilibrium diagram for Boudouard reaction with excessive solid carbon available [21].

Within the furnace, it is assumed that MnO_2 is completely reduced to Mn_2O_3 before the Boudouard reaction is initiated. A high CO_2 reactivity of the coke combined with a low CO reactivity of the ore, will cause elevated consumption of energy and coke, as well as a high CO/CO_2 ratio of the off-gases and fumes.

Alkaline elements have a catalyzing effect on the Boudouard reaction, causing the reaction to commence when the temperature reach 800ºC, if alkaline elements are present. Especially potassium has a catalytic effect.

If the temperature dependent equilibrium is reached, the CO_2 formed during reduction of the higher manganese oxides will re-react with sold carbon and CO (g) at temperatures approaching 800ºC [1]. However, Aderbigde & Szekely discovered the rate to be insignificant at temperatures below 950ºC [22]

2.3 Water-gas shift reaction

The water-gas shift reaction is an important step in many industrial processes, including production of ammonia and hydrogen. It is a reversible, exothermic, equilibrium controlled reaction, described by reaction (5) [23].

$$H_2O\ (g) + CO\ (g) = H_2(g) + CO_2(g) \qquad \Delta H^o_{1273} = -32.3 \frac{kJ}{mol}\ (5)$$

In a syngas atmosphere, i.e. an atmosphere consisting of CO, CO_2, H_2 and/or H_2O, the Water Gas Shift Reaction (hereafter WGSR) will determine the partial oxygen pressure if it reaches equilibrium [24].

A catalyst such as Fe or Cu is often required for the reaction to proceed. Due to this, and the factum that it is often difficult to know the exact content of the different components in the syngas, it is hard to tell if the WGSR reaches equilibrium. If equilibrium is not reached, the respective CO-CO_2 and H_2-H_2O reactions will determine p_{O2}.

Lower temperatures favor a shift to the right, or higher concentrations of the products in equation (5). When the temperature exceeds 800ºC, the equilibrium shifts to the left [25].

The water gas shift reaction will catalyze the reduction with hydrogen inside the particle when carbon, hydrogen and oxygen is present, meaning that the primary reduction agent will be hydrogen gas [26].

2.4 Reduction of the higher manganese oxides

The higher manganese oxides MnO_2, Mn_2O_3, Mn_3O_4 are compounds with more oxygen than manganese present. These oxides are easily reduced to a lower oxide or MnO, while the final reduction of MnO to metallic manganese is harder to achieve. Kinetics, thermodynamics, reducing agents and p_{O2} are all influencing the reduction process, and further discussed in this chapter.

2.4.1 Spontaneous reduction

MnO_2, Mn_2O_3, Mn_3O_4, are unstable oxides, and may reduce to lower manganese oxides spontaneously, when the temperature is elevated in air [1]; Gibbs energy for equation (6) becomes zero when the temperature reaches 485ºC, calculated with data from HSC chemistry 7.18Z. The spontaneous reduction of MnO_2 will thus proceed at this temperature in agreement with thermodynamic equilibrium calculations. The spontaneous reductions will proceed as described in reaction (6) -(8).

$$2MnO_2 = Mn_2O_3 + \frac{1}{2}O_2\ (g) \qquad \Delta H^0_{1273} = 80.6 \frac{kJ}{mol} (6)$$

$$3\ Mn_2O_3 = 2\ Mn_3O_4 + \frac{1}{2}O_2\ (g) \qquad \Delta H^0_{298} = 101.7 \frac{kJ}{mol}\ (7)$$

$$Mn_3O_4 = 3\ MnO + \frac{1}{2}O_2\ (g) \qquad \Delta H^0_{298} = 220.9 \frac{kJ}{mol}\ (8)$$

Gibbs energy will be zero for reaction (7) at 873ºC, and 2045ºC for reaction (8).

2.4.2 Kinetics

The kinetics of a reaction express at which speed the reaction will eventuate. Figure 5 below shows a schematic view of how the reduction of a manganese oxide particle may proceed in CO gas, corresponding to the shrinking unreacted core model.

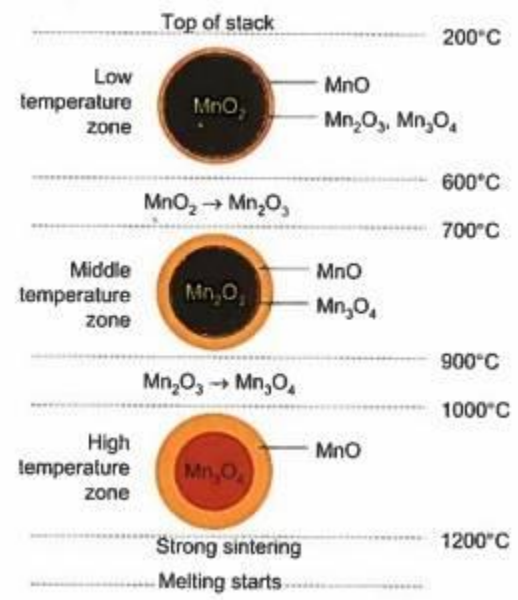

Figure 5: Schematic view of reduction of manganese oxide in CO gas [1].

The stepwise reduction starts at 200^{o}C on the surface of the particle, moving inwards to the center as the temperature increases.

2.4.3 Equilibrium reactions.

The reduction of the higher manganese oxides in a CO gas atmosphere are exothermic reactions, releasing energy. However, at elevated temperatures where the Boudouard reaction is initiated (above 800^{o}C), the total reduction will be endothermic because of the reversed Boudouard reaction. The reduction with CO gas takes place in the upper part of the furnace, contributing to heating the room tempered charge entering the furnace. These reductions take places per the following formulas;

$$2\, MnO_2 + CO\ (g) = Mn_2O_3 + CO_2\ (g) \qquad \Delta H^o_{1273} = -201\ \frac{kJ}{mol}\ (9)$$

$$3\, Mn_2O_3 + CO\ (g) = 2\, Mn_3O_4 + CO_2\ (g) \qquad \Delta^\circ H_{1273} = -179.9 \frac{kJ}{mol}\ (10)$$

$$Mn_3O_4 + CO\ (g) = 3\, MnO + CO_2\ (g) \qquad \Delta^\circ H_{1273} = -60.6 \frac{kJ}{mol}\ (11)$$

Hydrogen gas can also be used to reduce the higher manganese oxides, and has a greater reduction potential than CO-gas [24]. The reduction reactions are stated in reactions (12) -(14);

$$2MnO_2 + H_2\ (g) = Mn_2O_3 + \ H_2O\ (g) \qquad \Delta H^0_{1273} = \ -168.8\frac{kJ}{mol}\ (12)$$

$$3Mn_2O_3 + H_2\ (g) = 2Mn_3O_4 + \ H_2O\ \ (g) \qquad \Delta H^0_{1273} = \ -147.6\frac{kJ}{mol}\ (13)$$

$$Mn_3O_4 + H_2\ (g) = 3MnO + H_2O\ \ (g) \qquad \Delta H^0_{1273} = \ -28.3\frac{kJ}{mol}\ (14)$$

Lobo [24] found that hydrogen would cause a greater overall mass loss for manganese oxides when pure H_2 and nearly pure CO gas are compared.

One of the main advantages of using CO- gas instead of hydrogen gas is the effect of the Boudouard reaction. If there is solid carbon present, the Boudouard reaction will give a continuous supply of CO gas. If hydrogen gas where to be used, it must be supplied continuously. Hydrogen is also much more expensive than solid carbon, and often produced by the decomposition of methane gas.

From figure 6 it is observed that MnO_2 will reduce to Mn_2O_3 when the temperature reaches 510°C in air and the kinetics work at infinite speed. Mn_2O_3 will reduce to Mn_3O_4 when the temperature reaches 981°C, and α-Mn_3O_4 will reduce to β-Mn_3O_4 at 1190°C. Reduction to MnO will take place at 1652°C in air, where p_{O2}=0.2, market by 1 in figure 3 below, but further reduction to metallic manganese will not take place with an oxygen pressure this high [1].

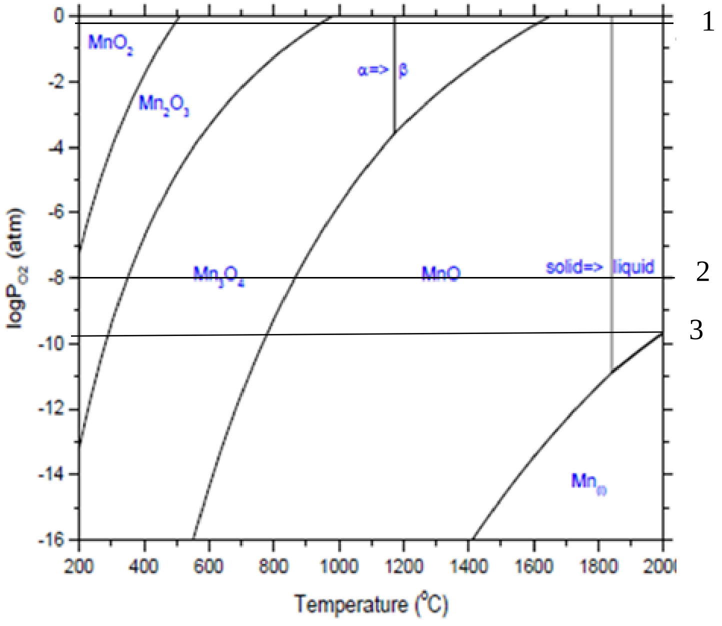

Figure 6:Phase diagram of reduction of manganese oxides, from [1].

Oxygen atmospheres with p_{O2} pressure equal to 10^{-8} is often used as for atmospheres made with inert gases, such as argon. The reduction temperatures can be seen by line 2 in figure 6. These temperatures are lower than those of line 1, but a reduction to metallic manganese will first take place when the p_{O2} is closer to 10^{-10}, shown by line 3.

2.5 Mechanisms for reduction

Manganese oxides can be reduced through different reduction mechanisms. Here are the shrinking unreacted core model, the grain model and Avrami equation looked on.

2.5.1 Shrinking unreacted core model.

The unreacted shrinking core model is based on a simple, layer-by-layer reaction progress. The assumptions made determines the simplicity of the model., but the foundation of the model is a material balance across the product layer the system is here considered isothermal, so that no heat balance or temperature dependencies of involved parameters need to be considered.

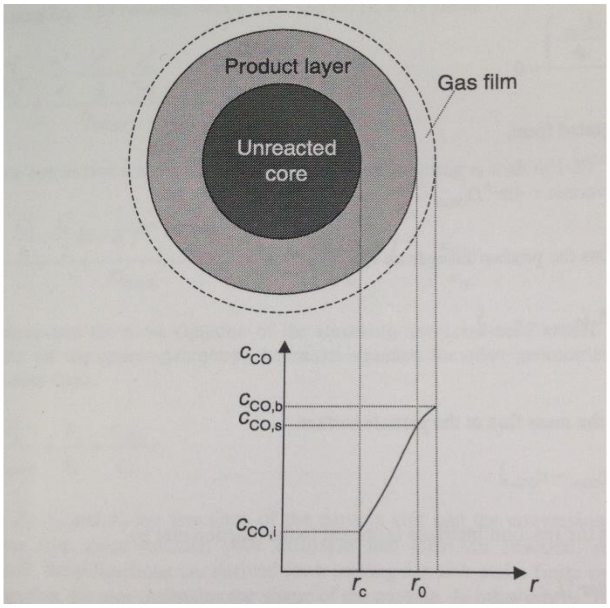

Figure 7: Shrinking unreacted core model view, concentration profile of the reactant gas, here CO gas [24].

Conversions vs. time relationships for porous and non-porous solids makes the base for the “law of additive reaction times”, which means that the time needed to complete a certain isothermal conversion is the sum of 1) the time needed during pure mass transfer control and 2) the time needed for the conversion under chemical control [27].

The main steps in the shrinking core reaction proceeds in five main steps [5];

1. Gas transport from bulk to the outer surface (gas-film resistance)
2. Gas diffusion through the porous metal layer to the unreacted pore (shell-layer resistance)
3. Chemical reaction between gas and solid oxide (interface resistance)
4. Outward gas diffusion through the metal layer (shell layer resistance)
5. Transfer the products from the outer surface to the bulk (gas-film resistance)

2.5.2 The grain model

The grain model assumes that the porous solid is made up of uniformed sized, smaller, non-porous grains, where each grain reacts consonant with the chemically controlled unreacted shrinking core model. This model is generalized and restrictive, but has been the groundwork for newer, more realistic models [28].

2.5.3 Avrami equation

The Avrami equation, or *JMAK equation*, express the fraction of material transformed at a given time in terms of nucleation and growth rate of the process. A small amount of a new phase is formed from the matrix. It is applied for isothermal reactions [29].

$$X(t) = 1 - e^{\left(-x_c(t)\right)} \; (X)$$

3 Experiments

11 experiments were in total executed, 5 of them were heated in argon, and the remaining 6 were heated in argon and then purged with methane gas. Some samples were further treated for and studied in an electron probe microscope

3.1 Materials

The manganese ore used is COMILOG ore, mined in Moanda, Gabon. It was delivered to Trondheim from ERAMET Porsgrunn august 2016. Properties of the ore can be seen in table 1.

Table 1: Chemical analysis of COMILOG ore done by ERAMET and SINTEF Mosjøen.

Element	**COMILOG ore [wt %]** **ENPRV124105**
H_2O	10.12
MnO	3.63
MnO_2	73.95
Fe_2O_3	3.27
Fe	2.29
Mn-tot [%]	50.4
MnO_2	75.2
LOI 950°C [%]	15.6

The ore used in the experiments were crushed to a size between 5-10 mm, the ore is showed in picture 1 below.

Picture 1: Untreated COMILOG ore

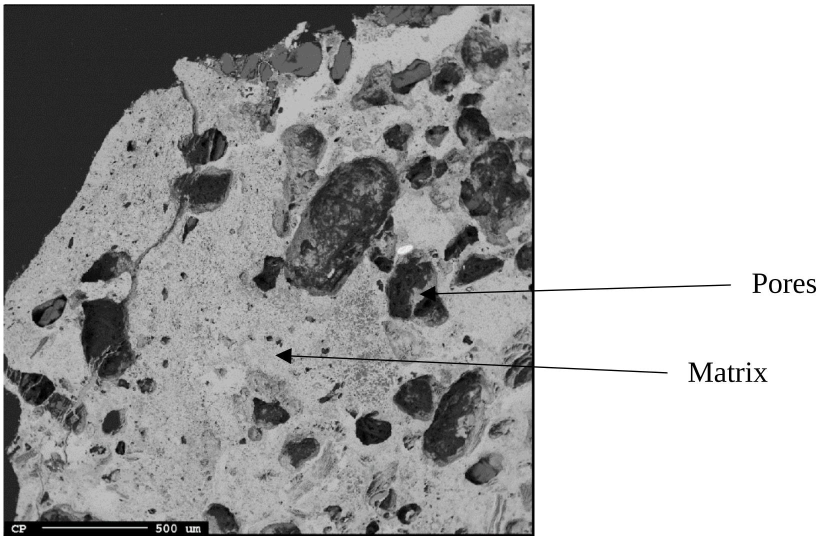

When studied in the electron probe microscope, the ore showed to be quite porous, making it difficult to take representative pictures and analyzes of the particles.

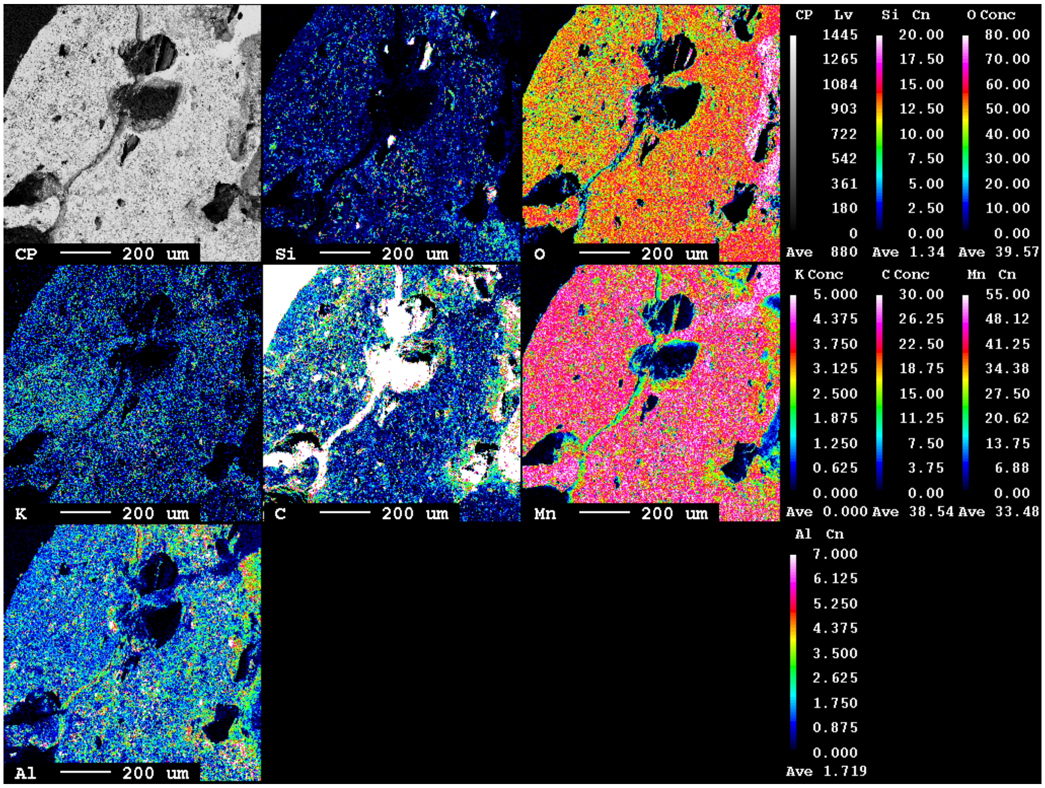

Picture 2: X-ray picture of untreated manganese ore.

The x-ray in picture 2 tells that the untreated ore has a uniform distribution of aluminum, manganese and oxygen, and that the ore is relatively complex.

Table 2: Analyzing points taken from the outskirts moving towards the center of the sample

No.	Si [wt%]	O [wt%]	K [wt%]	C [wt%]	Mn [wt%]	Al [wt%]	Total
1	0.849	38.723	0.758	2.286	53.386	1.777	97.779
2	0.697	36.275	0.575	4.08	50.169	2.06	93.856
3	1.354	37.252	1.274	3.805	48.042	3.214	94.941
4	0.994	38.919	1.571	1.994	52.258	1.685	97.421
5	0.583	38.459	1.045	2.252	52.583	1.411	96.333
Average	0.9	37.9	1	2.9	51.3	2	

Argon and methane were used as purging gases in the experiments. They had both a purity of 5.0, meaning they were 99.999% pure.

3.2 Equipment

The experiments were done with an ENTECH 1800 furnace. It is an induction furnace with a maximum operation temperature on 1450ºC, with heating elements made of SiC. It is controlled by Eurotherm 2408, which communicates with a program made in LabVIEW, RH2. RH2 makes program profiles, where signals from Eurotherm 2408 and the wall temperature, crucible temperature and effect measured by a thermoelement collection box (from national instruments) is logged. The temperatures are measured in the bottom of the thermoelement, and on the inside of the walls of the furnace.

The purging gas is fed in by mass flow controls from Alicat Scientific, and is operated on a display on each MFC.

The furnace was used to heat up a crucible with the manganese ore inside it, illustrated by figure 8, where a side-view of the furnace with crucible and thermocouple is displayed.

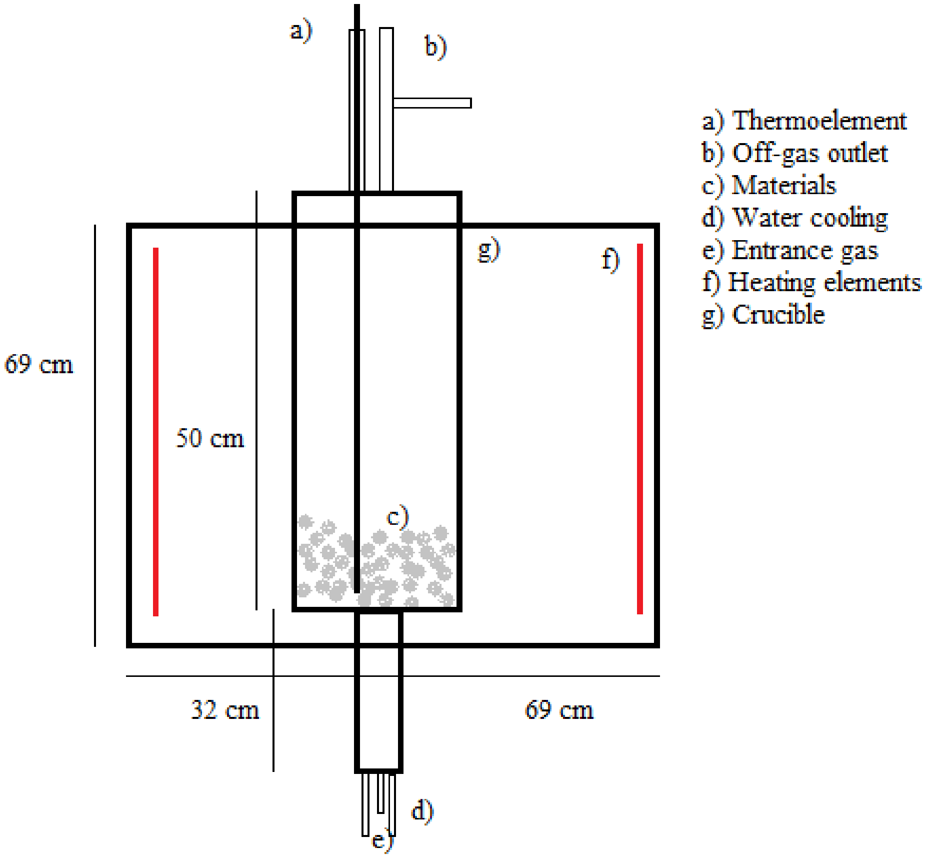

Figure 8: Side view of furnace with crucible inside.

The crucible is made of high carbon steel, and has dimensions OD/ID/H - 0.5/10.4/50 cm. The gas is purged in from the bottom, in a cylinder with water cooling to avoid heating of the gas before entering, as seen at e) and d) in figure 8. A lid is fastened on the top with six screws where the fumes and off-gases are released, as well as the thermocouple being inserted into the crucible. The height of 1000 g ore is approximately 10 cm inside the crucible.

The thermoelement used is a S type thermocouple, which is used for high temperature applications, and has a high accuracy and stability [30]. It is placed inside a protective ceramic tube, and consists of platinum rhodium – 10 % Pt. The thermocouple is placed almost centered in the crucible, and only the bottom part was in touch with the manganese.

It was attempted to find the distribution of heat inside the crucible when the furnace is running. This was done by heating the furnace up, and then pulling the thermocouple out, pausing every 5 cm to measure the temperature at said spot. The results can be seen in figure 9.

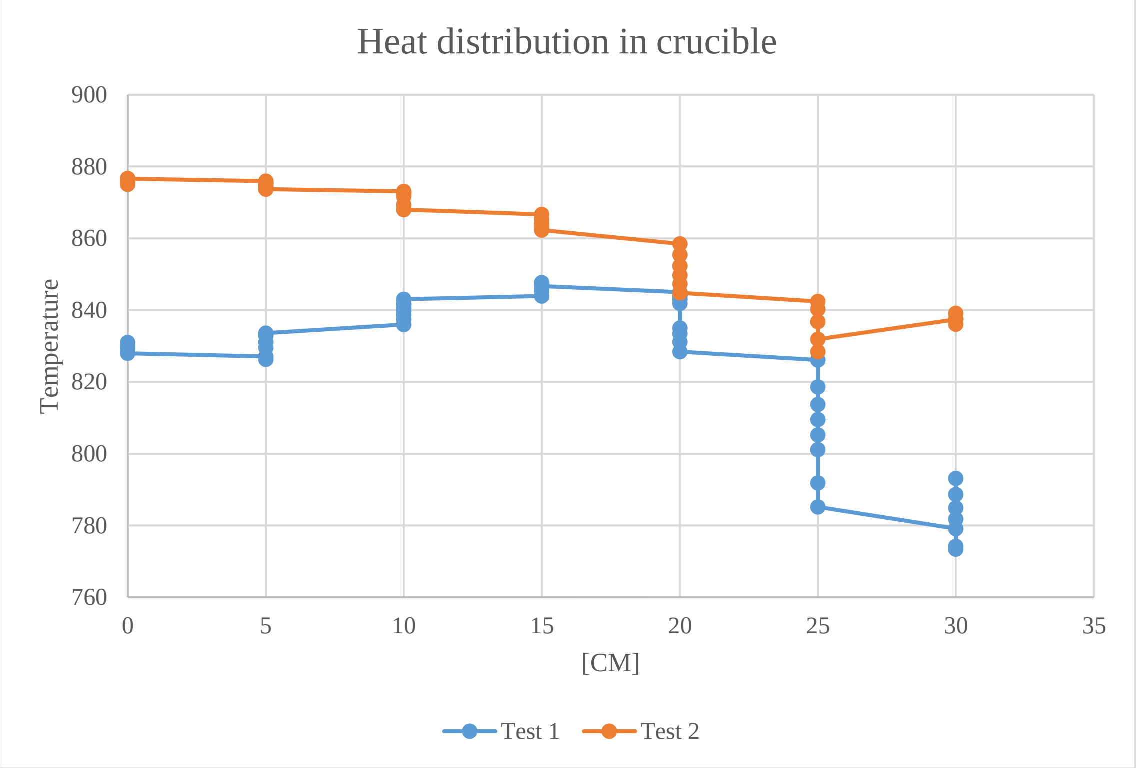

Figure 9: Heat distribution in crucible, 0 CM is the bottom.

Samples that were to be examined in an electron probe microscope were polished down to 1 µm by an automatic polishing machine, SAPHIR 550.

The samples were looked at in a field emission electron probe microanalyzer, model JEOL JXA-8500F. The JXA-8500F is a high performance thermal field emission electron probe micro analyzer combining high SEM resolution with high quality X-ray analysis of submicron areas.

3.3 Methods

The COMILOG ore was crushed and sieved to achieve a size distribution between 5 and 10 mm. Remaining dust were removed prior to experiments by rinsing it in tap water after the amount that were to be used in the experiment had been weighed.

The crucible was placed in the ENTECH furnace, and water cooling and gas tubes were fastened at the bottom of the crucible. The ore was poured inside the crucible, and the lid was fastened on top with screws. The thermoelement were inserted into the crucible through a pipe on the lid. The fan and water cooling were turned on, and the purging of argon gas was initiated. The furnace was thereafter turned on, and consequently the heating of ore commenced.

The reduction process is divided into non-isothermal and isothermal reduction. Non-isothermal reduction take place when the temperature is not constant, thus when the ore is heated. The temperature remains constant in an isothermal process [31], in other words when the ore is kept at a constant temperature.

Argon was purged through the crucible whilst the ore was heated to the predetermined temperature, at a rate 1.15 L/min, with ramping time 35ºC/min. An overview of the experiments that were conducted can be seen in table 3 below.

The samples starting with an A are samples that are only heated in only argon. The samples that starts with a C are purged with methane.

Table 3: Overview of conducted experiments. The samples starting on A were performed in argon, C were conducted in methane

Material	Sample #	Temperature [ºC]	Purging gas	Holding time	Mass [g] before	Mass [g] after
COMILOG ore	A1	500	Ar	none	200	190
COMILOG ore	A2	700	Ar	none	200	179
COMILOG ore	A3	1000	Ar	none	200	172.5
COMILOG ore	A4	1080	Ar	none	200	169
COMILOG ore	A5	1080	Ar	none	724	567
COMILOG ore	C1	700	CH_4	1 hour	200	166
COMILOG ore	C2	850	CH_4	1 hour	1000	762
COMILOG ore	C3	950	CH_4	1 hour	1000	795
COMILOG ore	C4	~900	CH_4	1 hour	1000	784
COMILOG ore	C5	1020	CH_4	1 hour	1000	803
COMILOG ore	C6	1070	CH_4	1 hour	1000	797

3.3.1 Purging with argon

When the predetermined temperature was reached, the furnace was turned off, and the crucible with ore was left in the furnace to cool, with purging gas still turned on. When the temperature was below 200ºC, the gas was turned off, and crucible with ore inside was left to cool in the furnace overnight.

After that, ore sample was removed from the crucible, weight loss registered, and the particles inspected visually. Some samples were further treated for examination in an electron probe microscope.

3.3.2 Purging with methane

After the initial heating step with argon as purging gas, argon is switched with methane, having a flow rate of 4.6 L/min. The temperature was kept as stable as possible for one hour whilst methane was purged through the crucible. When the holding hour was over, the furnace was turned off, and the crucible were cooled with argon gas having a flow rate of 1.15 L/min, until the temperature was below 200ºC, then the gas was turned off.

The crucible with ore inside cooled in the furnace overnight, thereafter the ore sample was removed from the crucible. The sample were weighed again to record weight loss, and inspected visually for deposited carbon. Some of the samples were further treated for examination in an electron probe microscope.

3.3.3 Sample preparation for electron probe microscope

Some samples were examined in an electron probe microscope. These samples were prepared by casting two or particles of each sample in epoxy, in a 2.5 cm casting form. The samples where then polished down to 1µm in a SAPHIR 550 through 4 consecutively steps, 900, 600, 3 µm and 1 µm.

The samples were covered with a thin, conducting film of carbon. The samples were coated by thermal evaporation, where the sample to be coated and carbon is placed in an evacuated chamber, before high current is run through the carbon. The sides of the samples were covered with aluminum foil.

The samples were then examined in an electron probe micro analyzer, a JEOL JXA-8500F. Overview pictures were taken of each sample, and mass analyzes done in 5 different spots. An x-ray picture was taken of each sample.

4 Results

11 experiments were executed. A general overview of the different experiments has been given in table 3. In 5 of the experiments, manganese ore was only heated in argon atmosphere, to investigate if the ore reduce and if so, the extent of the reduction. 6 experiments were heated in an argon atmosphere and then purged with methane gas. The intention was to see if carbon from methane gas was deposited on the manganese ore's surface. The temperature was varied to find the temperature were the deposition was the most effective.

4.1 Reduction in Argon atmosphere

200 g samples of manganese ore were heated to respectively 500°, 700°C, 1000° and 1080°C. A sample of 724 g were also heated to 1080°C. Samples A1, A2, A3 and A5 where studied in the electron probe microscope.

In these experiments, the furnace power was controlled by the temperature in the wall of the furnace, i.e. the power adjusted itself to achieve the correct temperature in the furnace walls. The temperature was not turned off before the correct temperature was attained in the crucible.

4.1.1 A1 - 500° Argon

200 g of manganese were heated to 500°C, to see if spontaneous reduction took place at temperatures this low. When 500°C was reached, the furnace was then turned off, and the crucible with ore inside left within the furnace to cool.

A restart in the program when the temperature reached 400°C, cause the graph to start on 400°C instead of at 0°C.

Table 4: Data for sample A1

Material	Sample #	Temperature [°C]	Purging gas	Holding time	Mass [g] before	Mass [g] after
COMILOG ore	A1	500	Ar	none	200	190

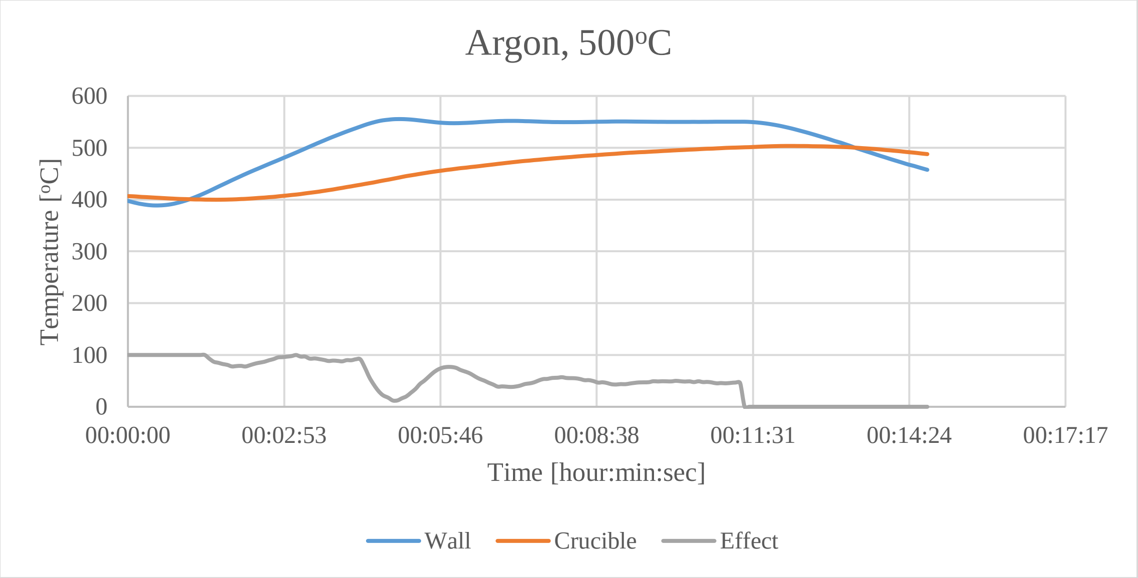

Diagram 1: Temperature development for sample A1 heated to 500°C.

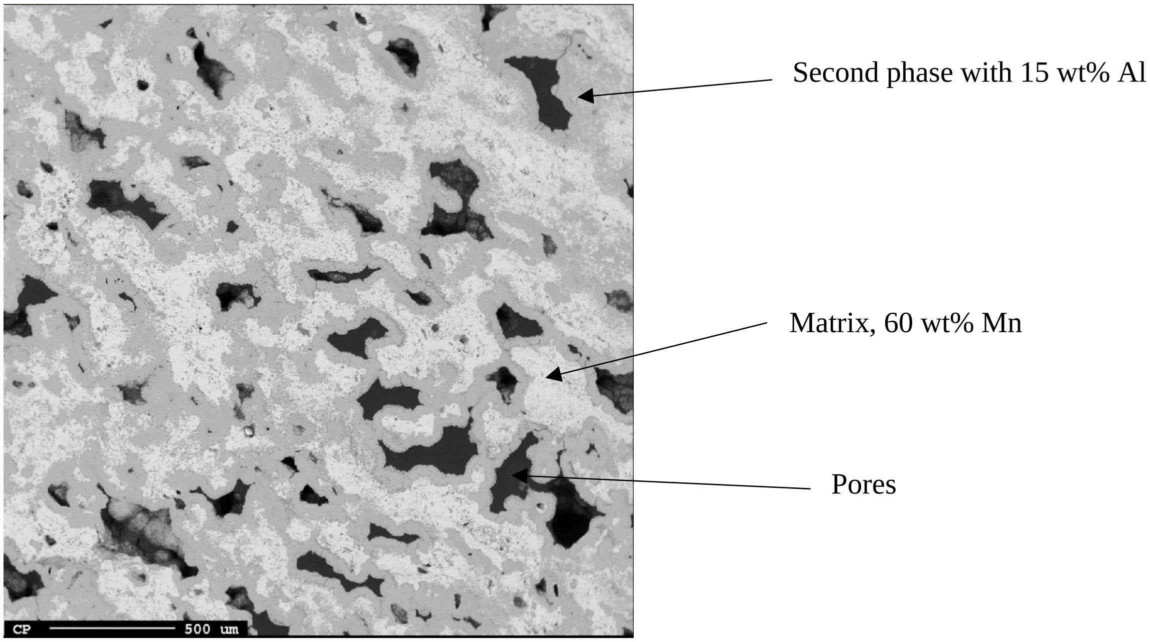

Picture 3: Manganese ore heated in argon to 500°C, sample A1

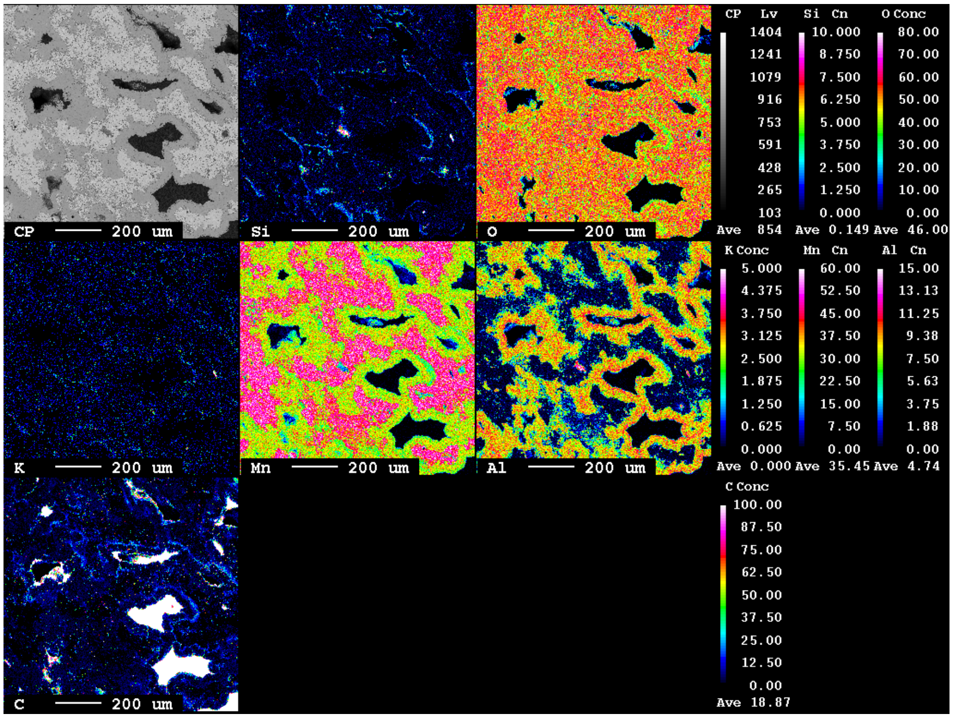

Picture 4: X-ray picture of manganese ore heated to 500°C, sample A1

The dark areas surrounding the pores and surface of the ore contains a higher amount of Al and 20 wt% less Mn than the matrix material.

Table 5: Mass analysis of A1

No.	Phase	O [wt%]	Mn [wt%]	Al [wt%]	Total
1	Dark	40.9	41.4	15.1	97
2	Dark	39	41.5	14.6	95
3	Dark	40.9	39.9	15.4	96.3
4	Dark	38.7	39.5	16.5	94.7
5	Dark	39.3	41.3	14.7	95.4
Average		39.8	40.7	15.3	
6	Matrix	33.8	58.4	0.5	92.9
7	Matrix	37.2	60	0.3	97.6
8	Matrix	37.3	58.5	0.3	96.1
9	Matrix	36.7	59.7	0.3	96.7
10	Matrix	37.2	60	0.2	97.4
Average		36.4	59.3		

4.1.2 A2 - 700^{o} Argon

200 g of manganese ore were heated to 700^{o}C to see if spontaneous reduction had taken place, and the difference between A1 and A2. After 700^{o}C was reached, the ore was left to cool in the crucible overnight, before it was inspected.

A small spike in wall temperature and effect 30 minutes in is due to a necessary adjustment of the set temperature to achieve 700^{o}C in the crucible.

Table 6: Data for sample A2

Material	Sample #	Temperature [^{o}C]	Purging gas	Holding time	Mass [g] before	Mass [g] after
COMILOG ore	A2	700	Ar	none	200	179

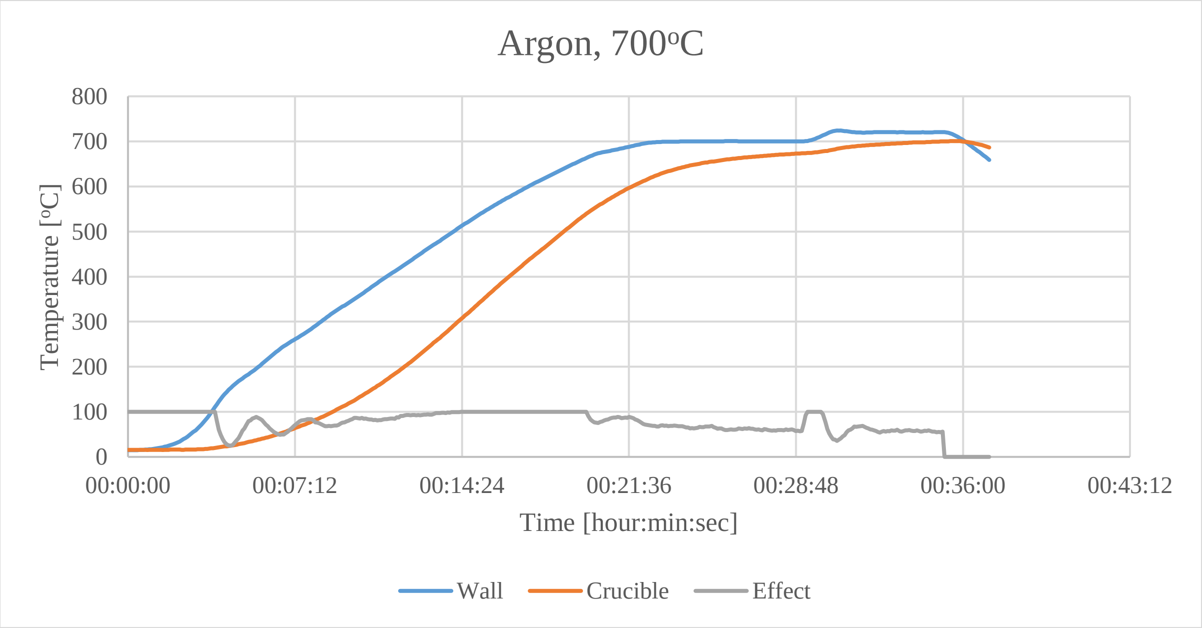

Diagram 2: Temperature development of A2, heated to 700^{0}C.

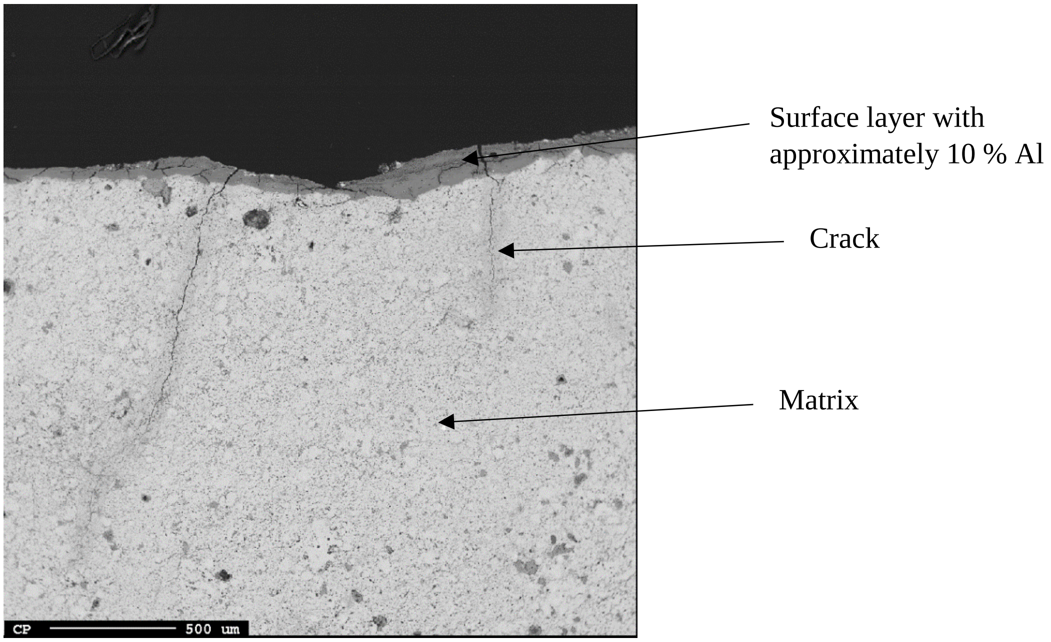

Picture 5: Manganese ore heated to 700°C, sample A2

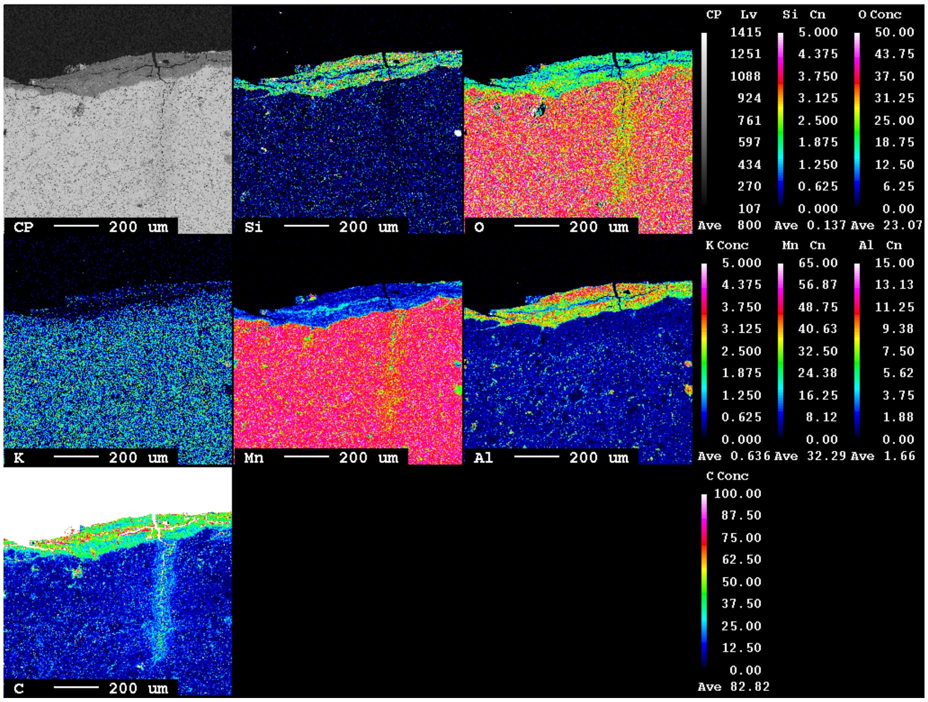

Picture 6: X-ray picture of manganese ore heated to 700°C, sample A2

There is a decreased oxygen content in the immediate surroundings of the crack in the particle, as well as a higher amount of carbon. The surface layer contains about 10 wt% Al, whereas the concentration is closer to 0 in the matrix.

Table 7: 21-25 were taken in the surface layer, 26-30 in the particle matrix.

No.	Phase	O [wt%]	Mn [wt%]	Al [wt%]	Total
21	Dark	22.381	7.804	15.646	49.931
22	Dark	23.499	7.111	16.882	52.607
23	Dark	11.74	20.041	5.174	37.291
24	Dark	22.758	13.749	13.819	53.908
25	Dark	19.966	12.113	12.665	49.405
Average		22.2	10.2	14.8	
26	Matrix	28.583	61.688	0.931	92.34
27	Matrix	28.721	62.614	0.661	93.18
28	Matrix	27.976	59.713	1.182	90.184
29	Matrix	26.237	56.512	1.911	86.186
30	Matrix	27.696	62.248	0.975	91.522
Average		27.8	60.6	1.1	

4.1.3 A3 - 1000^{o}C Argon

200 g of manganese ore were heated to 1000^{o}C, to find the amount of reduction caused by heat at 1000^{o}C. After 1000^{o}C was reached, the furnace was turned off, and the ore cooled in the crucible overnight, before it was inspected visually.

Table 8: Data for sample A3

Material	Sample #	Temperature [^{o}C]	Purging gas	Holding time	Mass [g] before	Mass [g] after
COMILOG ore	A3	1000	Ar	none	200	172.5

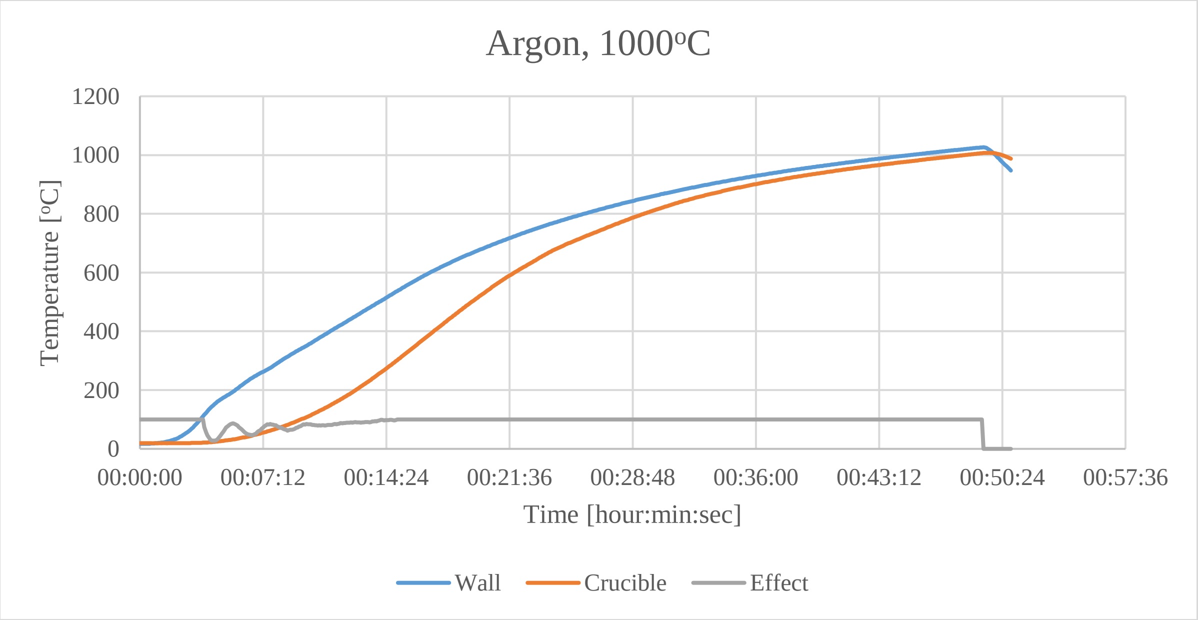

Diagram 3: Temperature development of sample A3, heated to 1000^{o}C..

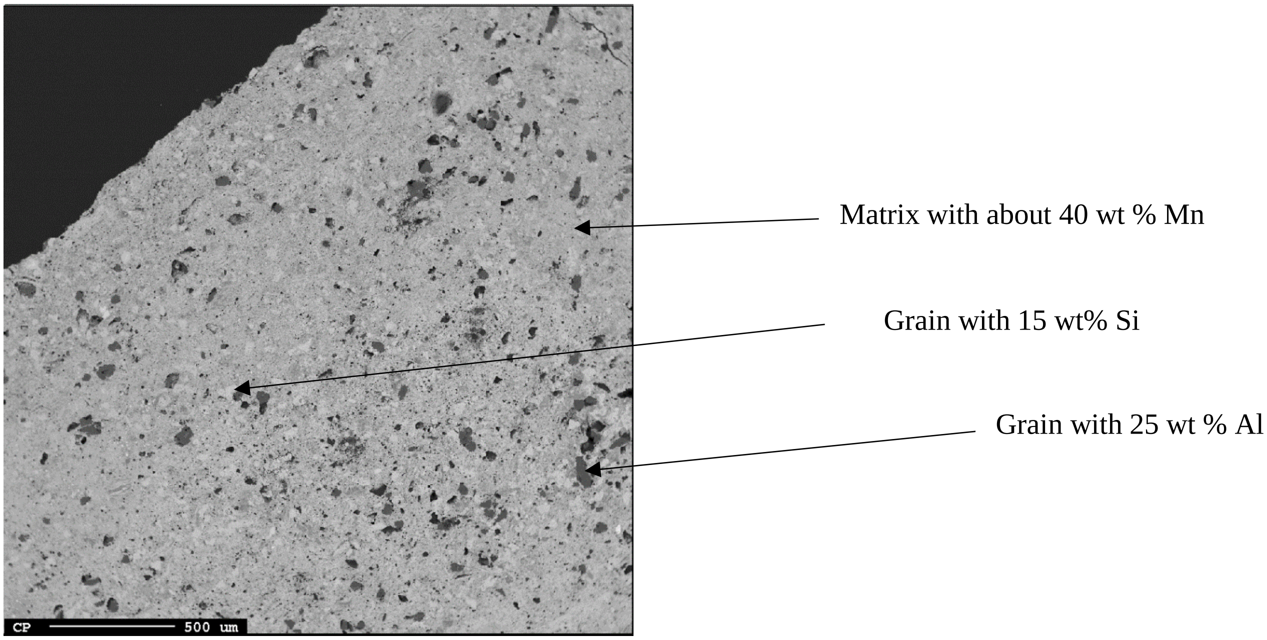

Picture 7: Manganese ore heated to 1000ºC, sample A3

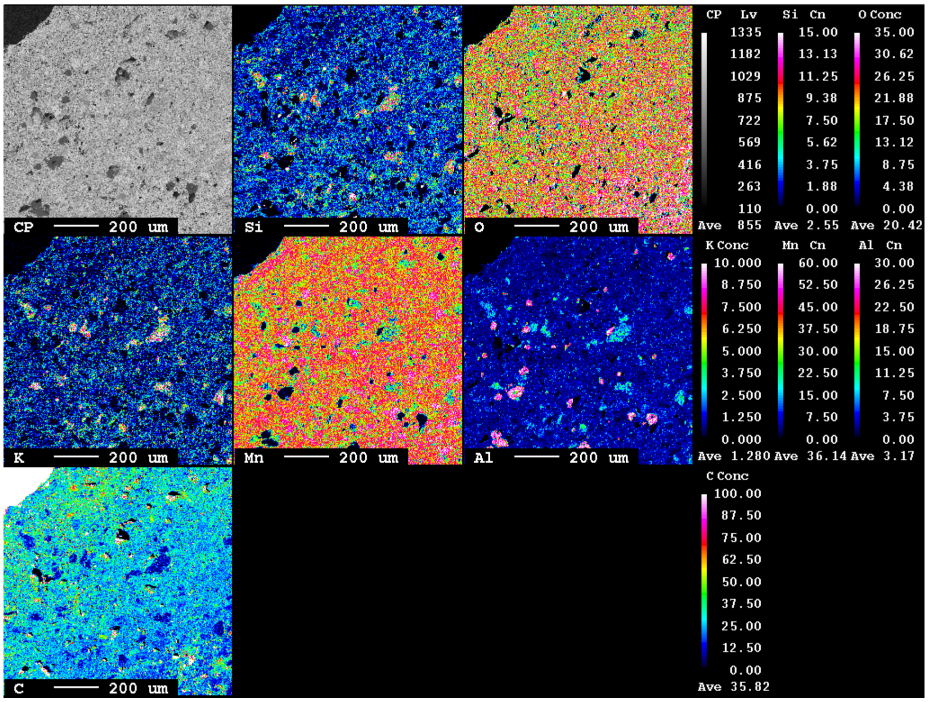

Picture 8: X-ray picture of manganese ore heated to 1000ºC, sample A3

Two types of grains are observed in the matrix, a darker grain with a low amount of manganese and about 25 wt % Al and almost white grains with approximately 15 wt % Si.

4.1.4 A4 – 1080ºC Argon

200 g of manganese ore was heated to 1080ºC, to find the maximum amount of reduction that could have happened for the experiments executed in this report. The furnace was turned off when 1080ºC was reached, and the crucible with ore inside left to cool overnight.

Table 9: Data for sample A4.

Material	Sample #	Temperature [ºC]	Purging gas	Holding time	Mass [g] before	Mass [g] after
COMILOG ore	A4	1080	Ar	none	200	169

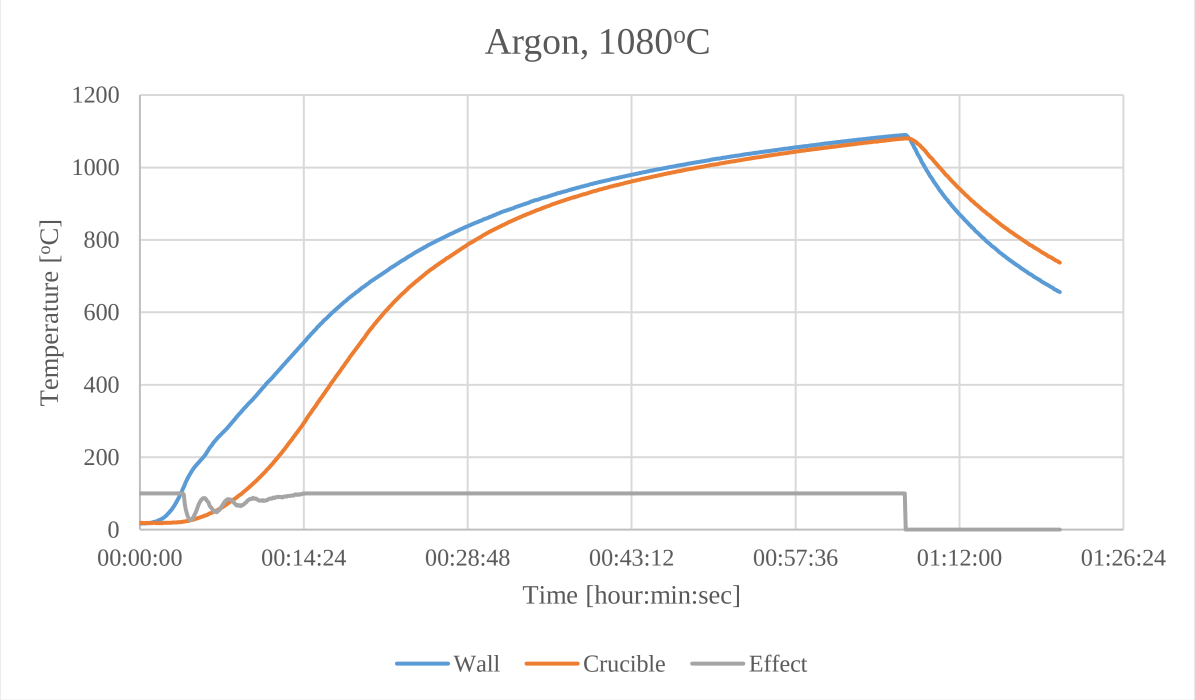

Diagram 4: Temperature development of sample A4 heated to 1080ºC.

4.1.5 A5 – 1080^{o}C Argon

724 g of manganese ore were heated to 1100^{o}C in the crucible, and then left to cool overnight. The amount of ore was increased to have comparable results with the ore purged with methane, with a mass of 1000 g. However, a lack of ore in the right size caused the amount to be reduced to 724 g were used.

Table 10: Data for sample A5

Material	Sample #	Temperature [^{o}C]	Purging gas	Holding time	Mass [g] before	Mass [g] after
COMILOG ore	A5	1100	Ar	none	724	567

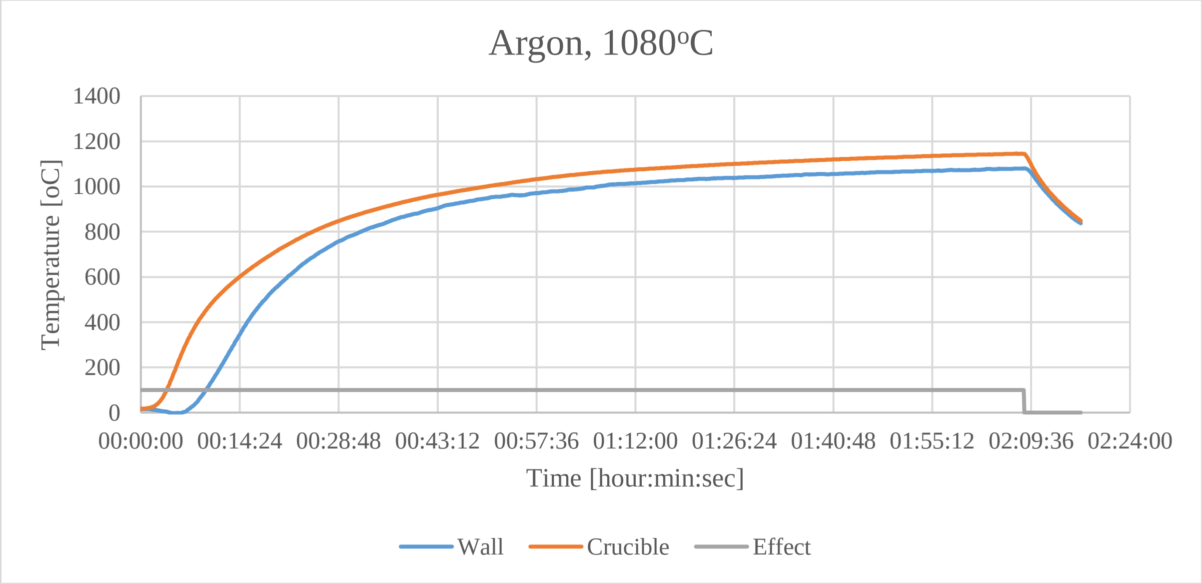

Diagram 5: Temperature development of sample A5, heated to 1080^{o}C.

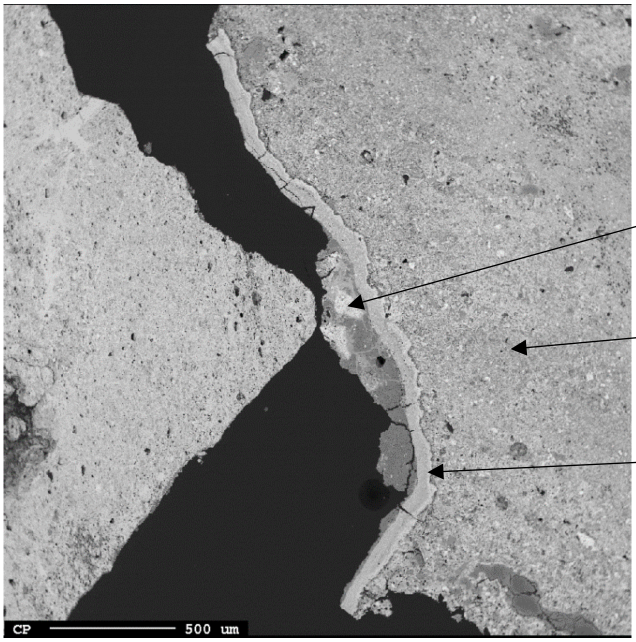

Layer found on particle, appear to have fallen off on most of the surface

Matrix with 35 wt % Mn

Innermost surface layer

Picture 9: Manganese ore heated to 1080^{o}C, sample A5

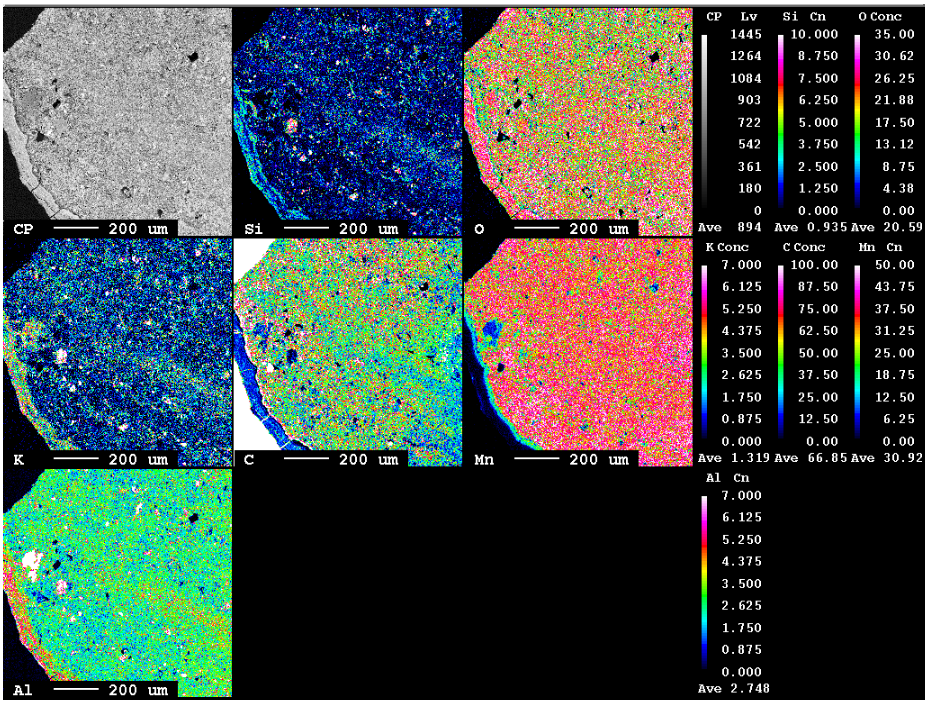

Picture 10: X-ray picture of manganese ore heated to 1080ºC, sample A5

The layer on the surface has an increased amount of aluminum and reduced amount of manganese compared to the rest of the particle. Content of carbon is also significantly lower than the matrix. The surface layer and the ore particle contains approximately the same amount of oxygen.

Table 11: Analyzing points are taken from the outside, point 1 being in the surface layer, moving towards the center.

No.	O [wt%]	Mn [wt%]	Al [wt%]	Total
1	35.5	1.3	4.9	51.528
2	27.2	41.6	4.4	87.526
3	35.4	29.7	9.5	99.374
4	24.8	41.1	3.8	85.945
5	26.99	44.3	5.2	89.377
Average	26.33	42.3	4.46	

4.2 Reduction and deposition with methane

6 samples of ore were heated to respectively 700^{o}C, 850^{o}C,900^{o}C, 950^{o}C, 1020^{o}C, 1080^{o}C while argon (1.15 L/min) gas was purged through the crucible. The flow of argon was then turned on, and methane was purged through the crucible, 4.6 L/min, for one hour. The ore was then cooled inside the crucible while argon gas was purged through at 1.15 L/min until the temperature was below 200^{o}C. Samples C1, C3, C5 and C6 were studied in the electron probe microscope.

4.2.1 C1 - 700^{o}C CH_4

This experiment was designed to figure out the lowest temperature possible to deposit carbon. As no carbon was deposited on the ore, lower temperatures were not tested.

Black dot indicates the beginning of purging with methane. A temperature increase is observed immediately after the start of purging. No carbon flakes were observed ascending from the crucible during the experiment, but humid off-gases ascended from the crucible for a short period after methane purging were commenced.

Only 200 g of manganese ore were used in the experiment, but to have comparable results to the work done in the course TMT 4500 [10] the amount is increased for the rest of the experiments with methane, giving an equal contact time of the methane on the ore for the experiments.

Table 12: Data for sample C1

Material	Sample #	Temperature [^{o}C]	Purging gas	Holding time	Mass [g] before	Mass [g] after
COMILOG ore	C1	700	CH_4	1 hour	200	166

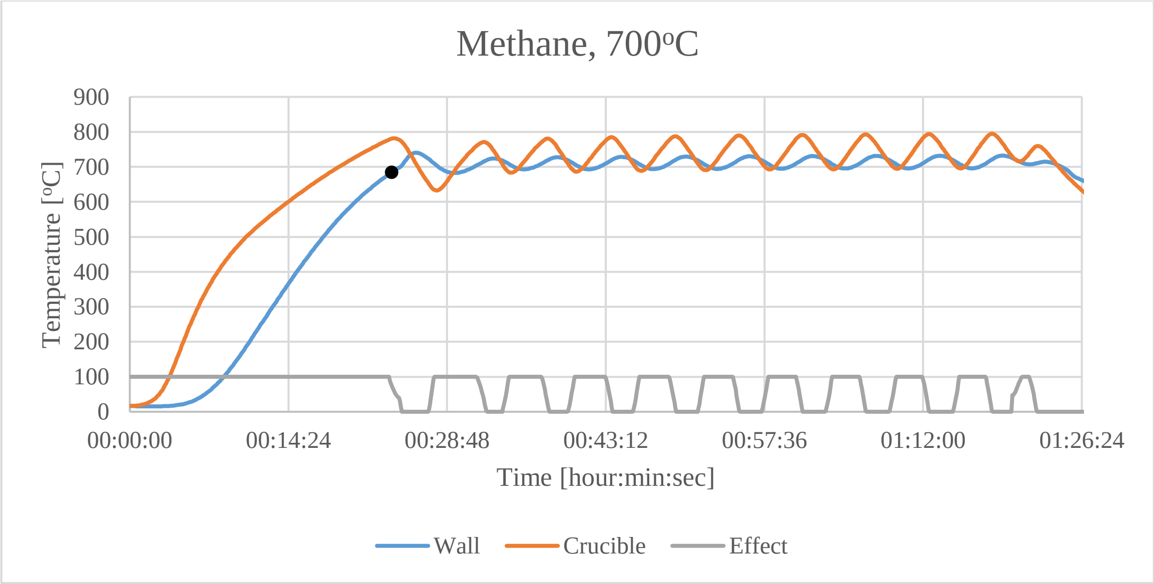

Figure 10: Temperature development for sample C1. Black dot indicates start of methane purging through the crucible.

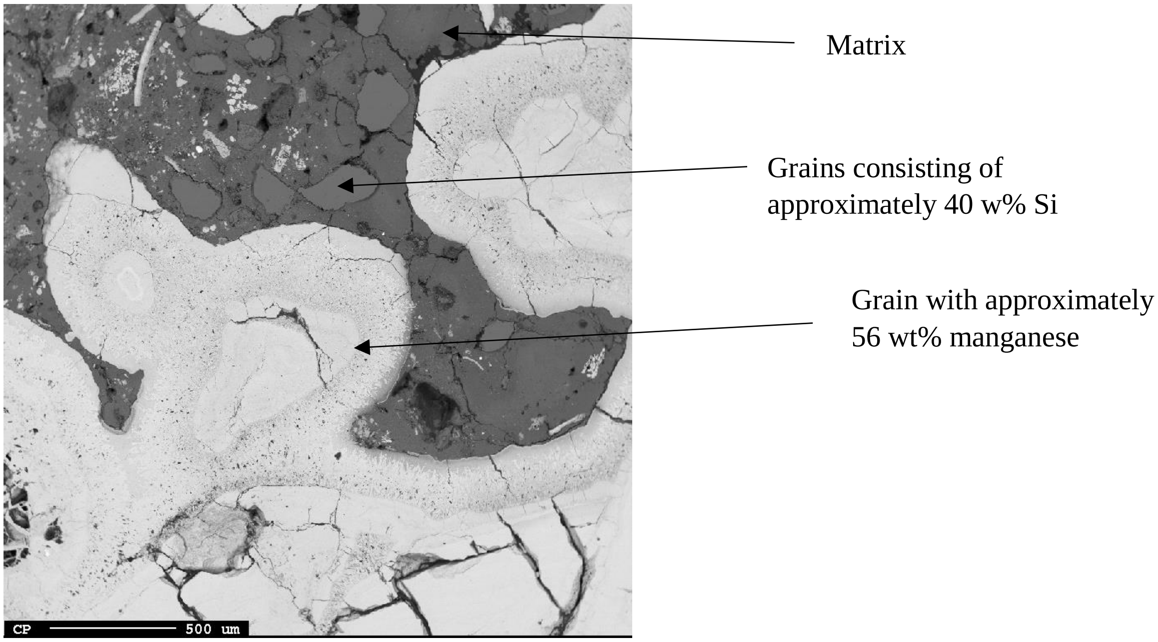

Picture 11: Manganese ore heated to 700ºC, sample C1

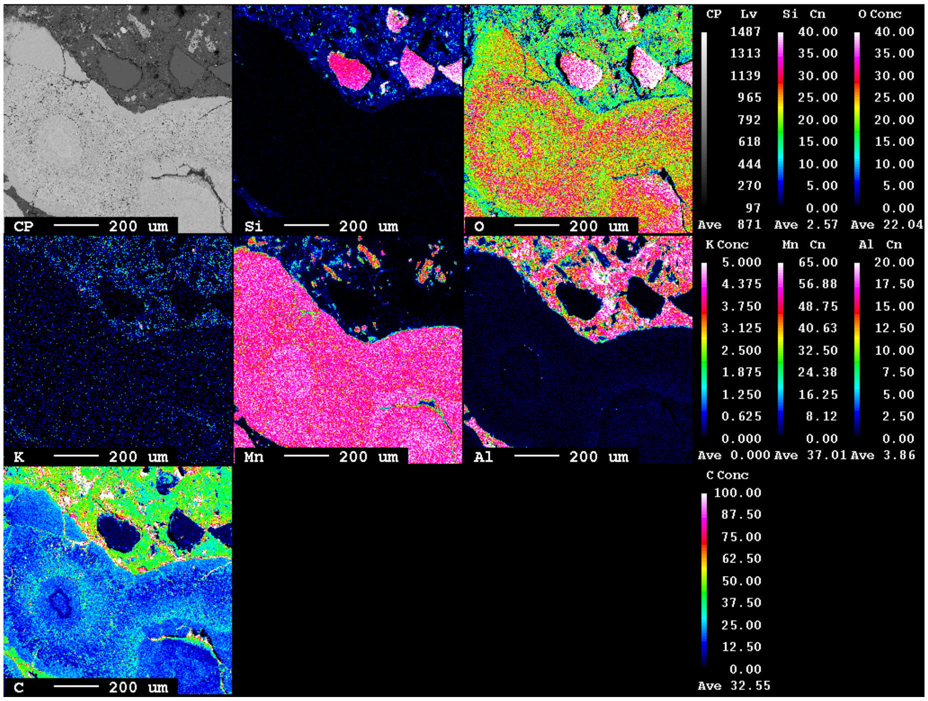

Picture 12: X-ray picture of manganese ore exposed for methane gas at 700ºC, sample C1

Table 13: 11-15 are taken of the matrix, 15-20 of the light particle.

No.	Phase	Si [wt%]	O [wt%]	Mn [wt%]	Al [wt%]	Total
11	Matrix	44.746	49.283	0.163	0.031	94.223
12	Matrix	44.214	49.441	0.1	0	93.755
13	Matrix	4.889	26.544	0.473	23.489	55.92
14	Matrix	7.502	27.718	0.222	23.786	59.975
15	Matrix	0.014	19.414	64.081	0.424	83.965
Average		25.33775	34.48	0		
16	Light grain	0.031	22.039	64.727	0.272	87.121
17	Light grain	0	19.36	66.394	0.232	85.986
18	Light grain	0.075	25.846	66.543	0.244	92.708
19	Light grain	0.014	19.326	67.397	0.214	86.985
20	Light grain	0.076	19.538	65.391	0.214	85.232
Average		0	21.2218	66.0904	0	

4.2.2 C2 – 850ºC CH_4

1000 g of ore were heated to 850ºC. The temperature was chosen to check for influence of the Boudouard reaction on deposition of carbon. Humid off-gas ascended from the crucible simultaneously with the increase in temperature after the purging with methane was started. The ore was then left to cool in the crucible overnight. No carbon was deposited.

Table 14: Data for sample C2

Material	Sample #	Temperature [ºC]	Purging gas	Holding time	Mass [g] before	Mass [g] after
COMILOG ore	C2	850	CH_4	1 hour	1000	762

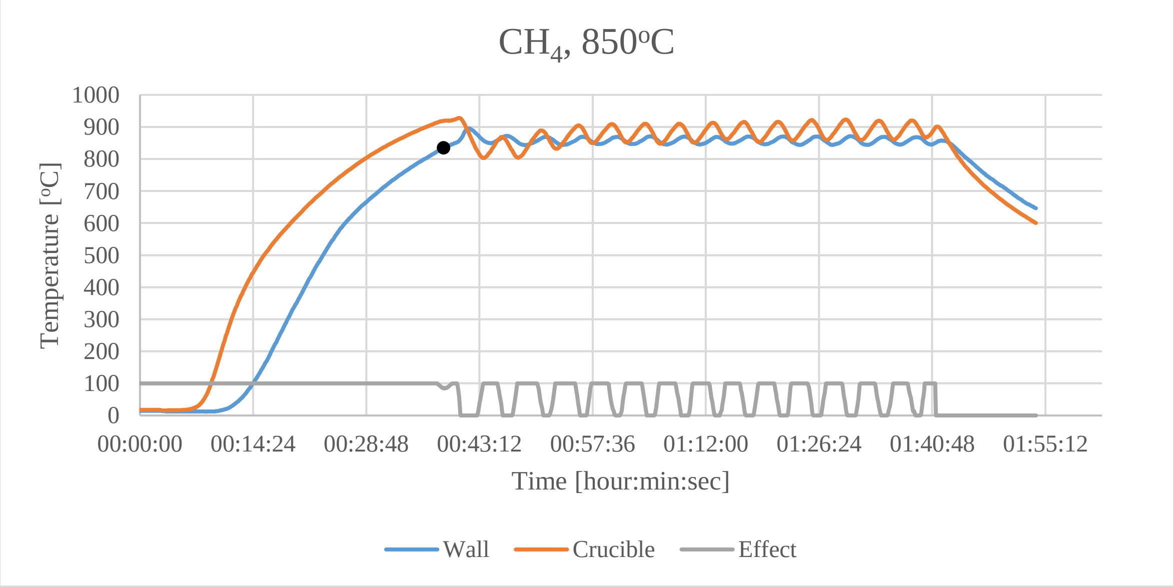

Diagram 6: Temperature development for sample C2. Black dot indicates the commence of purging of methane.

4.2.3 C3 - 950^{o}C CH_4

The sample was heated to 950^{o}C to look at the difference between sample C2 heated to 850^{o}C. Humid off gasses ascended from the crucible at the same time the temperature spiked when methane was purged through the crucible. After the purging was finished, the ore was left to cool overnight. A small amount of carbon was deposited on the ore.

The spike of the wall temperature 23 minutes in is due to adjustments of the thermocouple, and the spike 38 minutes in is due to switching of the wires, making the power sent to the furnace be adjusted after the temperature in the furnace. There is a possibility that the temperature is higher than registered, due to trouble with the furnace.

Table 15: Data for sample C3

Material	Sample #	Temperature [^{o}C]	Purging gas	Holding time	Mass [g] before	Mass [g] after
COMILOG ore	C3	950	CH_4	1 hour	1000	795

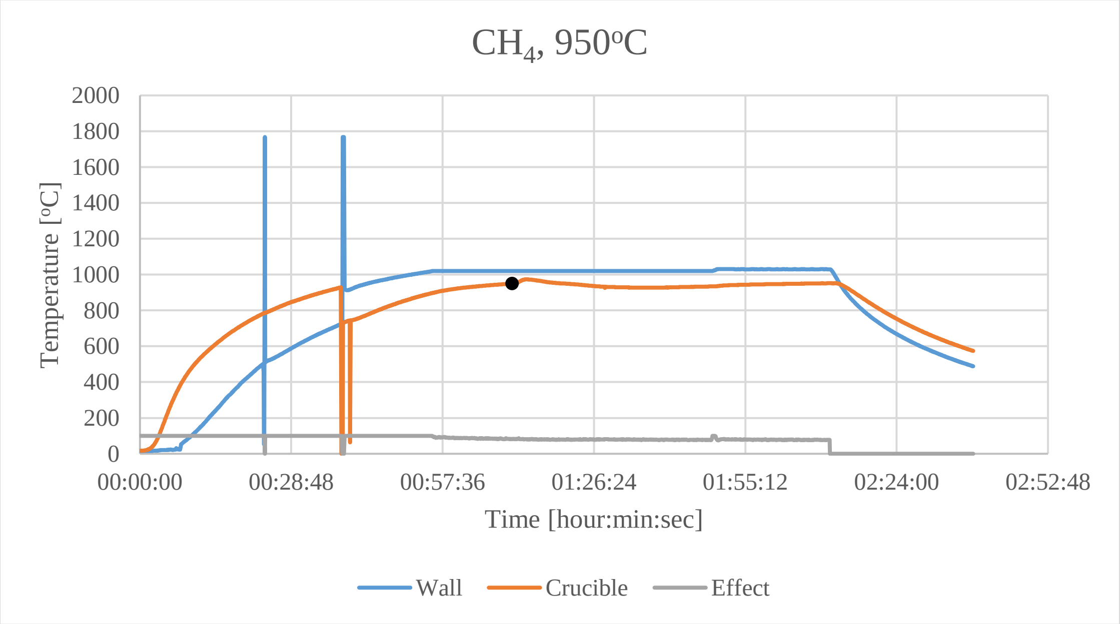

Diagram 7: Temperature development for sample C3. Black dot indicates the beginning of purging with methane.

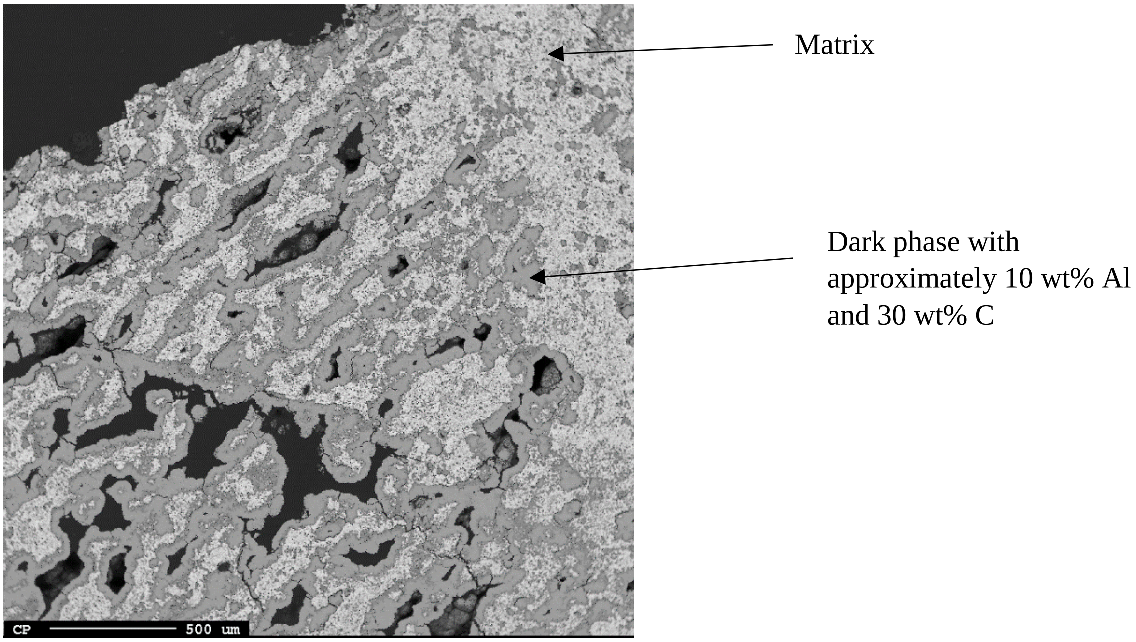

Picture 13:Manganese ore heated to 950°C, sample C3

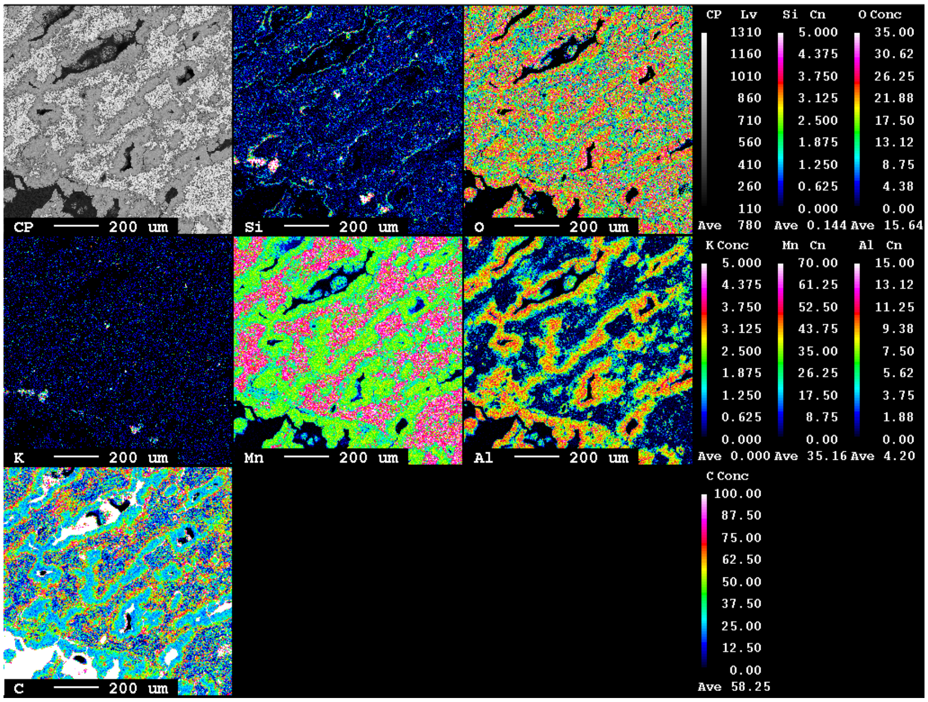

Picture 14: X-ray of manganese ore heated to 950°C, sample C3

There seem to be more oxygen present in the darker phase around the edges and pores than in the matrix. Around 40 wt% Mn is present in the darker phase, compared to 70 wt% in the matrix. There seem to be 30 wt% carbon in the dark phase.

Table 16: 31-35 is done in the darker phase, 36-40 in the matrix.

No.	Phase	O [wt%]	Mn [wt%]	Al [wt%]	Total
31	Dark	22.385	40.908	15.286	79.733
32	Dark	21.668	39.295	15.336	77.213
33	Dark	21.906	42.791	15.27	80.119
34	Dark	21.989	40.71	15.909	78.727
35	Dark	21.085	40.043	15.013	76.342
Average		21.8	40.7	15.36	78.4
36	Matrix	19.926	72.725	0.175	92.932
37	Matrix	18.723	70.012	0.248	89.124
38	Matrix	18.027	69.595	0.247	88.022
39	Matrix	18.827	71.45	0.229	90.65
40	Matrix	19.197	72.548	0.26	92.124
Average		18.94	71.3	0	

4.2.4 C4 – 900^{o}C CH_4

The sample was supposed to be heated to 1000^{o}C for comparison with results from the project written in TMT4500 [10]. After the purging of methane were commenced, an increase in temperature took place, accompanied by humid off-gases ascending from the crucible.

Trouble with the furnace and thermocouple throughout the experiment, caused spikes and sudden drops in the temperature. Purging of methane was commenced at 945^{o}C instead of the originally planned 1000^{o}C. The flask with argon gas ran empty during the experiment, meaning that the ore was not purged with argon during cool down. For these reasons, this sample is not relied much upon later.

Table 17: Data for sample C4

Material	Sample #	Temperature [^{o}C]	Purging gas	Holding time	Mass [g] before	Mass [g] after
COMILOG ore	C4	~900	CH_4	1 hour	1000	784

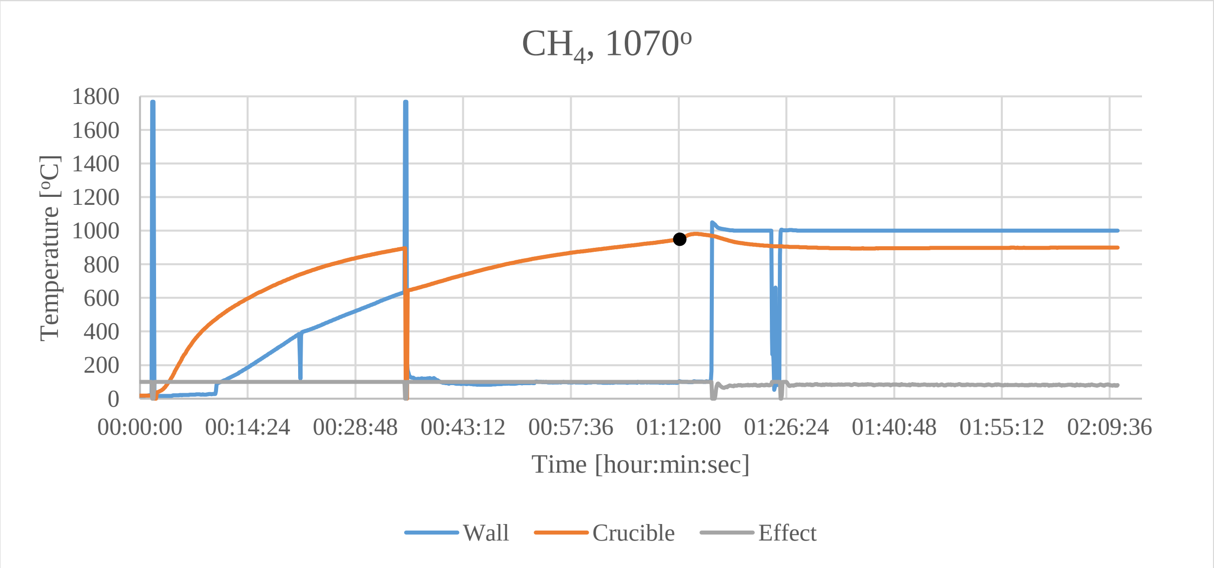

Diagram 8: Temperature development in sample C4. Black dot indicates the beginning of purging with methane.

4.2.5 C5 – 1020ºC CH_4

1000 g of manganese ore was heated to 1020ºC, to see if carbon would deposit on the oxide surface. The temperature did not increase when the purging of methane was commenced, nor was there any moisture in the off gas. When the purging was completed, the ore was left to cool overnight. Carbon was not deposited

The lack of spike in temperature when purging was commenced is likely caused by the ore having been heated to 800ºC in an earlier experiment, which had to be canceled before the purging with methane was started.

The temperature was originally planned to be 1000ºC, but the heating value was written in wrongly, causing the power not turn itself of when 1000ºC was reached.

Table 18: Data for sample C5

Material	Sample #	Temperature [ºC]	Purging gas	Holding time	Mass [g] before	Mass [g] after
COMILOG ore	C5	1020	CH_4	1 hour	1000	803

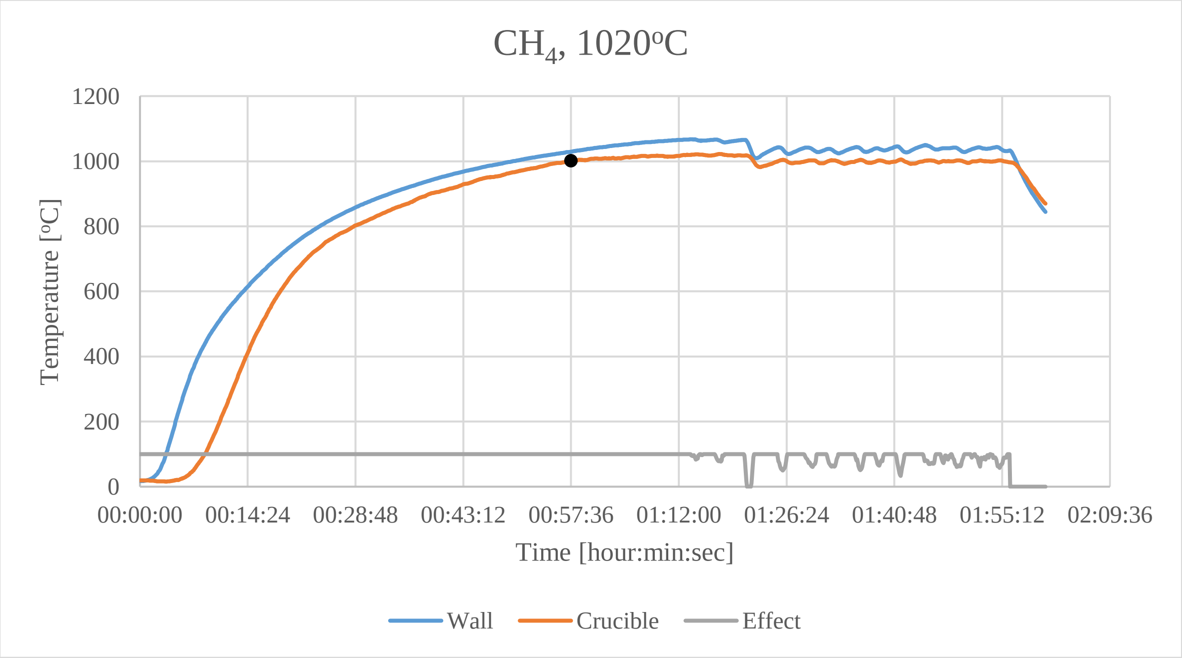

Diagram 9: Temperature in wall, crucible and effect plotted. Black dot indicates the start of CH_4 purging.

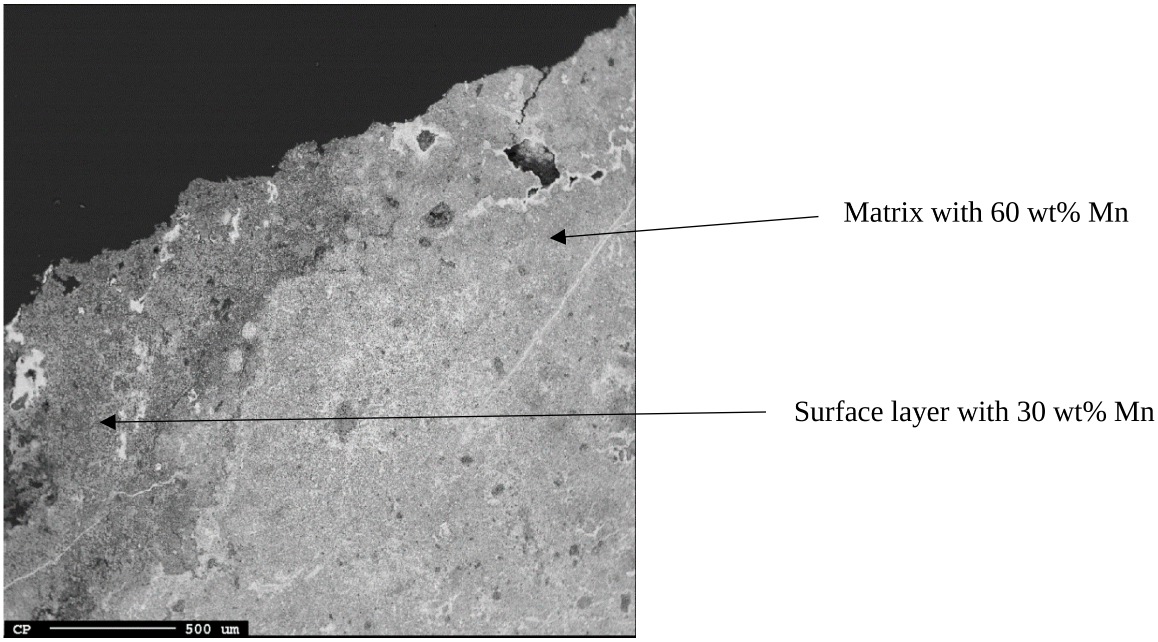

Picture 15: Manganese ore heated to 1020^{o}C, sample C5

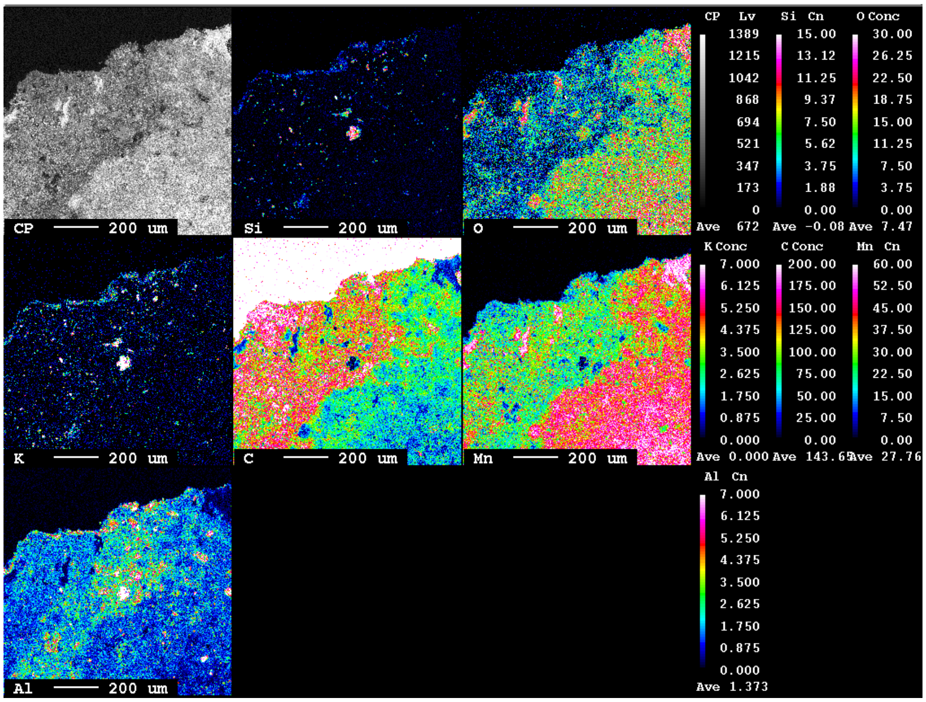

Picture 16: X-ray picture of manganese ore heated to 1020^{o}C, sample C5

The non-continuous surface layer contains a smaller amount of oxygen and higher amount of carbon than the rest of the particle. The matric contains a larger amount of manganese, while the amount of aluminum is uniform.

Table 19: Analyzing points have been taken from the outskirts of the sample moving to the center. 11 is taken in the surface layer.

No.	O [wt%]	C [wt%]	Mn [wt%]	Al [wt%]	Total
11	13.9	28.9	27.3	2.3	72.662
12	21.689	4.64	66.869	0.347	93.621
13	14.746	24.413	30.956	3.275	73.526
14	19.394	9.402	59.262	0.678	88.83
15	20.752	6.844	64.705	0.434	92.833
Average	20.6		63.58		

4.2.6 C6 – 1070ºC CH_4

Sample C6 was heated to 1070ºC, and the purging of methane commenced. The intention was to see if a temperature higher than 1000ºC had a positive effect on the deposition. It was purged for one hour before the ore was left to cool within the crucible in the furnace overnight. Carbon was deposited on the ore.

The temperature begun to decrease when purging was initiated, despite the power running at 100 %,

Table 20: Data for sample C6

Material	Sample #	Temperature [ºC]	Purging gas	Holding time	Mass [g] before	Mass [g] after
COMILOG ore	C6	1070	CH_4	1 hour	1000	797

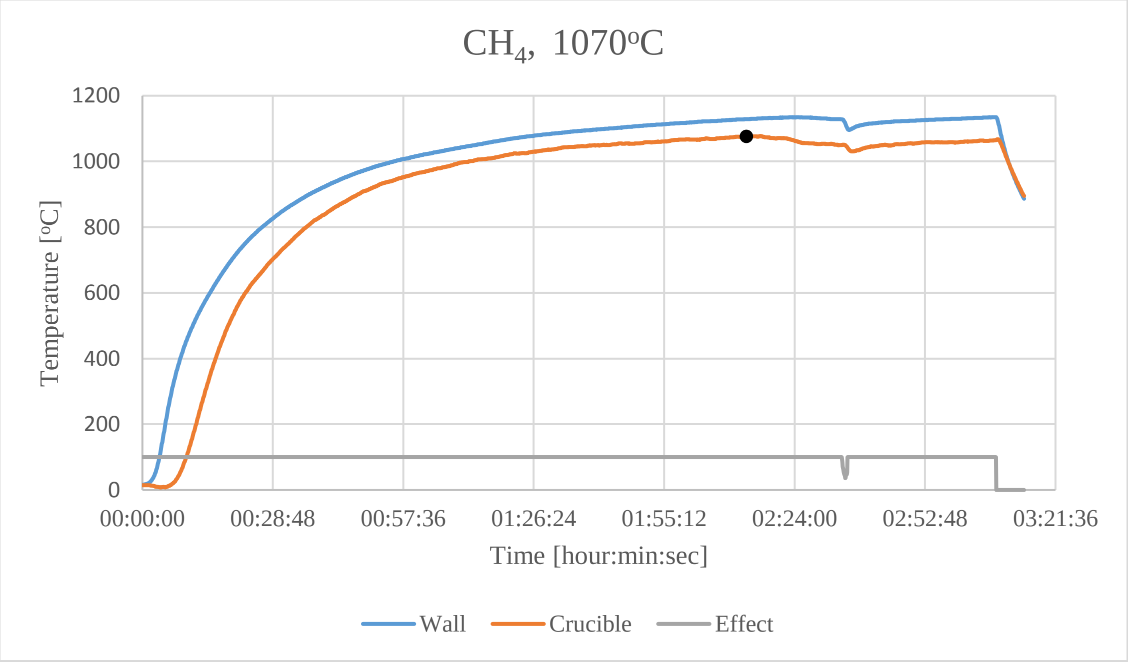

Diagram 10: Temperature development for sample C6. Black dot indicates when the purging of methane was commenced.

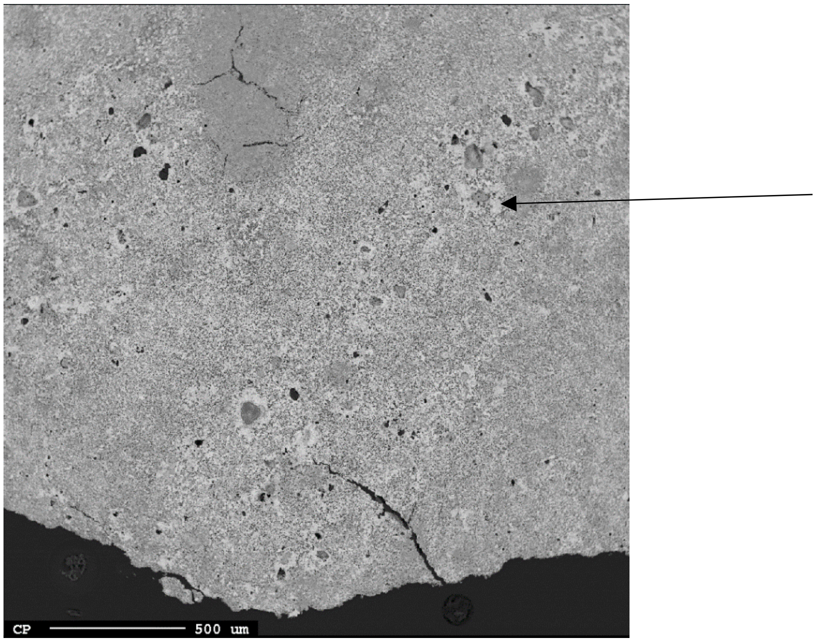

Matrix, about 50 wt% Mn

Picture 17: Manganese ore heated to 1020°C, sample C6

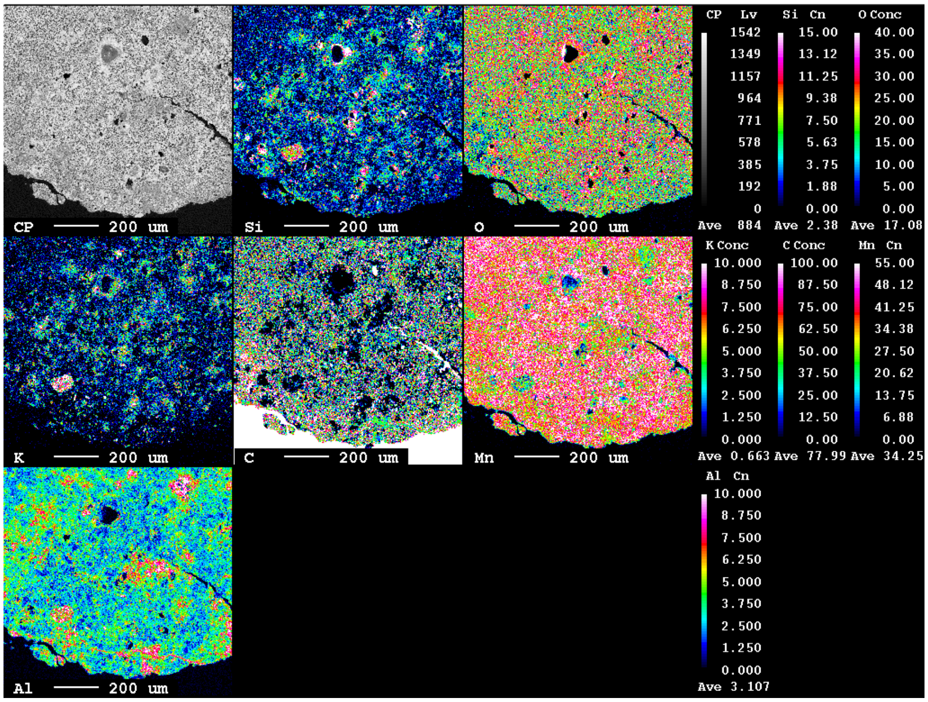

Picture 18: X-ray picture of sample C6

The matrix of the particle has an even distribution of the elements that were analyzed during x-ray. The oxygen concentration seems to be higher in the core of the particle. amount Carbon was deposited on the surface, but this is not seen in the pictures.

Table 21: Analyzing points are taken from the rind moving towards the center.

No.	Si [wt%]	O [wt%]	Mn [wt%]	Al [wt%]	Total
21	11.75	31.1	30	9.1	92.9
22	2.4	25.4	49.5	7.8	94.5
23	5.4	27.6	55.7	2.9	97.8
24	3.2	25.5	52.3	5.7	95.1
25	3.3	24.2	37.3	6.4	87.6
Average	3.6	25.7	45	6.4	

5 Discussion

11 experiments were executed, 5 samples were heated in argon, and 6 samples were heated in argon and then purged with methane. The effect of methane, deposition of carbon and reduction of the higher manganese oxides will be discussed.

5.1 Reduction of Mn ore in argon

Manganese ore was heated in argon to see if non-isothermal reduction took place, to look at reduction caused by heat, and reduction caused by methane. An overview of the 5 samples are shown in table 22 below, and the temperature evolvement is plotted in diagram 11.

Table 22:Overview of samples heated in an argon atmosphere.

Material	Sample #	Temperature [^{o}C]	Gas used	Holding time	Mas [g] before	Mass [g] after	[%] Reduction
COMILOG ore	A1	500	Ar	none	200	190	5 %
COMILOG ore	A2	700	Ar	none	200	179	10.5 %
COMILOG ore	A3	1000	Ar	none	200	172.5	13.8 %
COMILOG ore	A4	1080	Ar	none	200	169	15.5 %
COMILOG ore	A5	1080	Ar	none	724	567	21.6 %

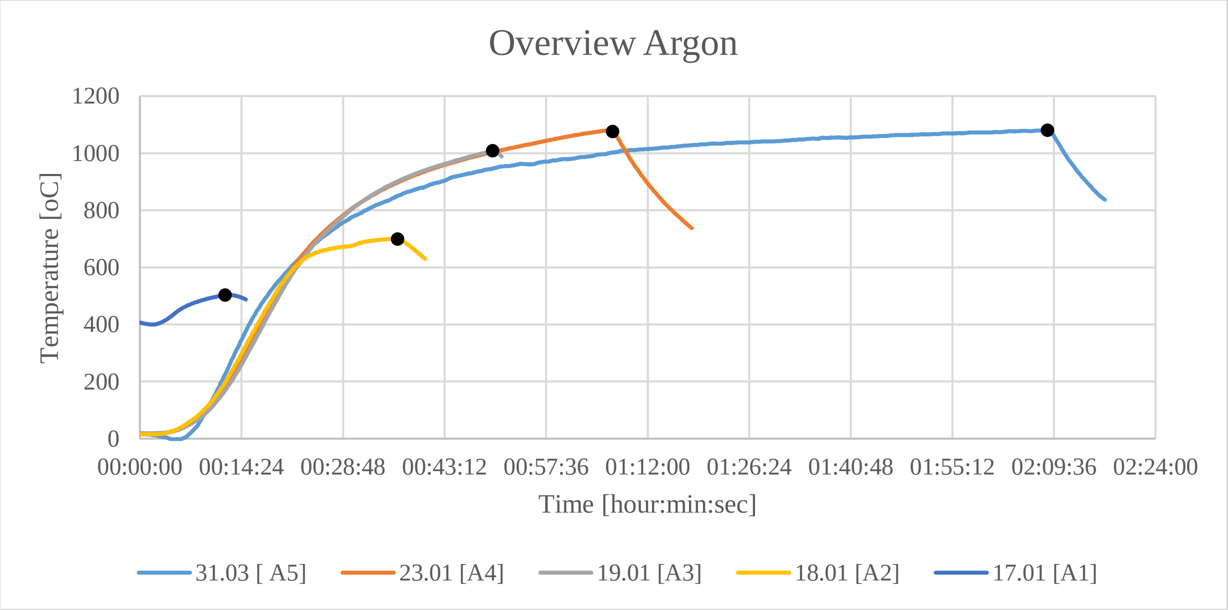

Diagram 11:Samples heated in Argon. Black dot indicates the time when pre-determined temperature was reached, and the furnace were turned off.

The reduction of mass is calculated and shown in table 22. In table 1, the original MnO_2 values of the ore is stated. The loss of mass is a more trustworthy source of information than the mass analysis done with the microprobe, as one particle cannot speak for the entire sample. Mass calculations were done, but these had oxygen values higher than possible in a manganese compound. Therefore, it is assumed that all loss of weight is a result of evacuation of oxygen in a MnO_2 compound, and that the conversion of MnO_2 is linked directly to the percentage of reduced mass. The result is plotted in diagram 12 below [32]. The trendline reveals an increasing conversion as the temperature the samples have been exposed to increases, in other words, the higher the temperature the ore has been exposed for, the more oxygen leaves.

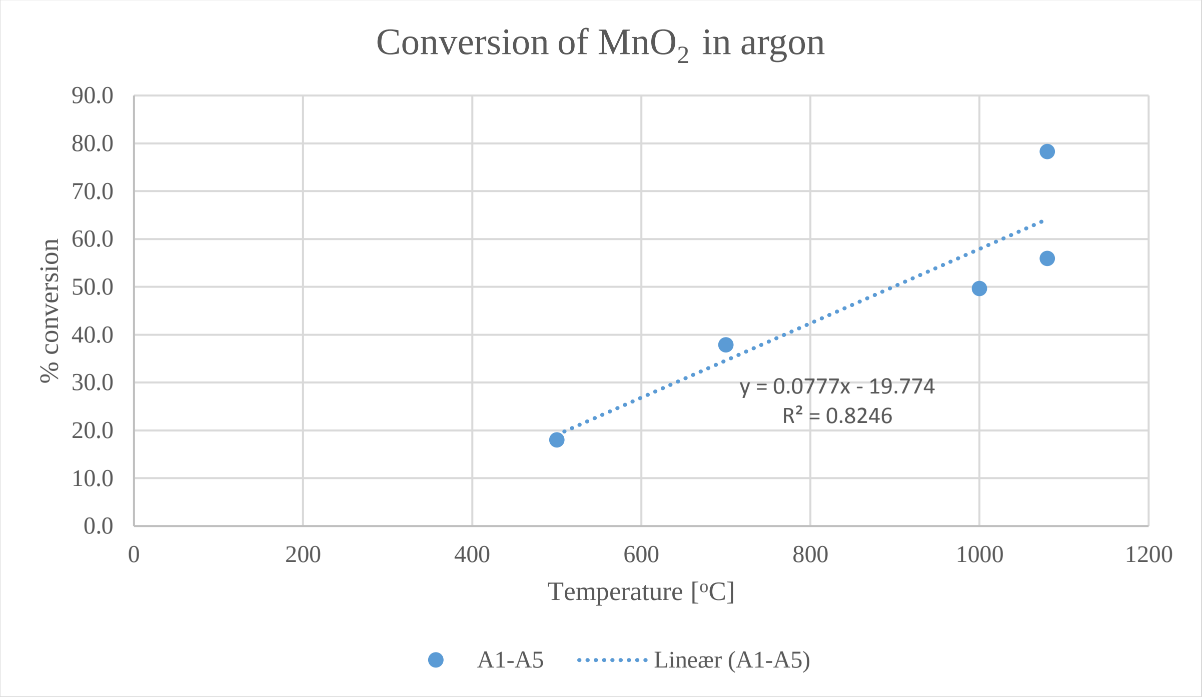

Diagram 12: MnO_2 conversion an increasing conversion is observed with increasing temperature, plotted in the trendline.

Picture 20 shows sample A1, A2, A3 and A5. A second phase can be observed on the surface and around pores in sample A1, and at the surface for samples A2 and A5. No surface layer was found in sample A3, which had a matrix structure dispersed with particle. Untreated manganese ore is displayed in picture 19 for comparison.

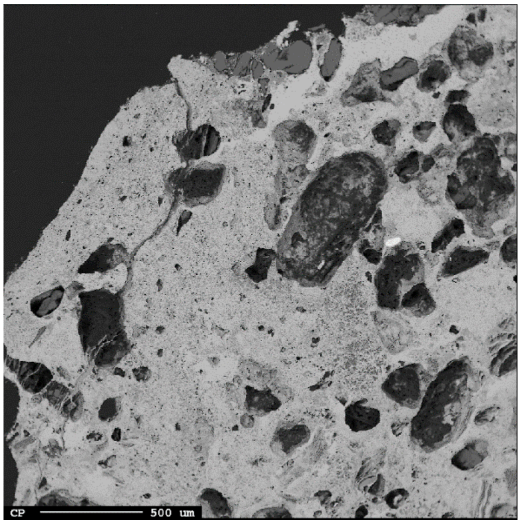

Picture 19: Untreated manganese ore for comparison.

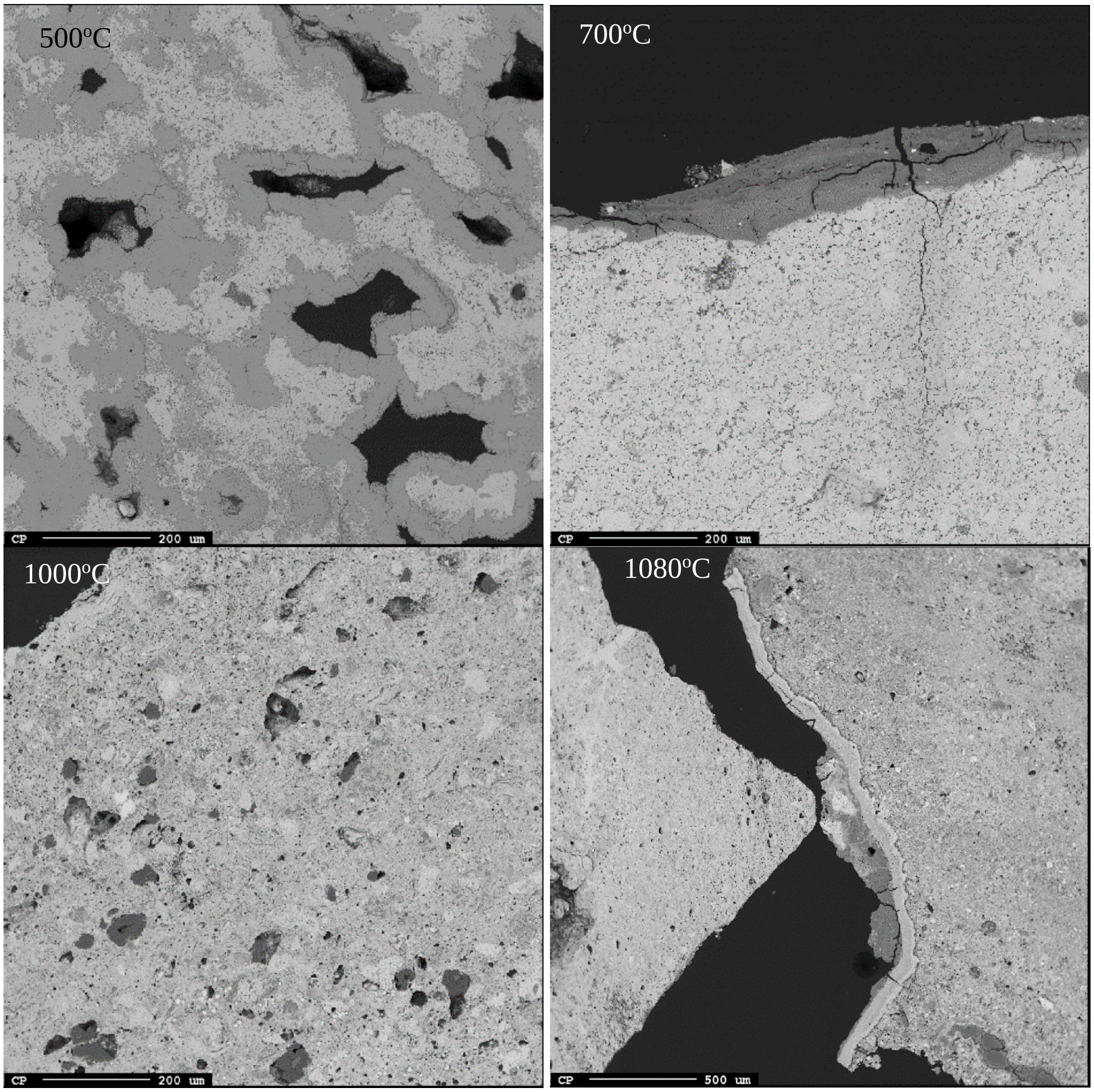

Picture 20: respectively from left; manganese ore heated to 500^{o}C (A1), 700^{o}C (A2), 1000^{o}C (A3) and 1080^{o}C (A5).

A1 was heated to 500^{o}C. Two phases are observed in the sample, a dark phase around the pores and along the surface, and a matrix phase. The darker phase contained about 15 wt% Al and 30 wt% Mn, while the matrix contained closer to 55 wt% Mn and almost no Al. From table 22 it is seen that the mass was only reduced with 5 wt%, so no major changes have taken place. A similar structure was found in sample C3, and these two structures are compared later.

Sample A2 was heated to 700^{o}C. The surface layer contains approximately 10 wt% Al and 10 wt% Mn, whereas the matrix contains around 55 wt% Mn and 1 wt % Al. The layer was not found around the entire particle. The concentration of oxygen was smaller around the crack in the particle, and the mass was reduced with 10.5 wt%.

A3 differ the most from the other samples heated in argon, as the matrix contains grains, and no layer on the surface. The darker grains contain 25 wt % Al, and the white grains contained 15 wt % Si. From the x-ray, picture 21, it seems that the concentration of oxygen is slightly higher towards the center of the particle. This comply with the shrinking unreacted core model, where the reaction starts at the particle surface and advance towards the particle center. The mas was reduced with 15.8 wt%.

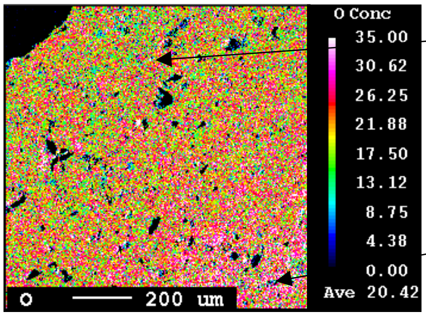

Approximate oxygen concentration of 20%

Oxygen concentration around 25-35%

Picture 21: x-ray of the oxygen concentration in sample A3, heated to 1000°C

Two surface layer on top of each other are observed in sample A5 heated 100°C. Only the innermost layer was analyzed. This layer had a 5 wt% concentration of Al and contained no Mn. The matrix contained around 40 wt% Mn and 4 wt% Al. This sample had the highest conversion of MnO_2, and the highest loss of mass of 21 wt%.

A diffusion pattern of the aluminum in the samples was not expected, but was observed. The aluminum appear to diffuse to the rind of the phase, and is, with an exception of sample A3, found on the surface of the particle. Because the structure differed in all the samples, it is difficult to say anything general about the movement or the influence of heat. Comparison of the x-ray analysis of Mn and Al are showed in picture 22 below.

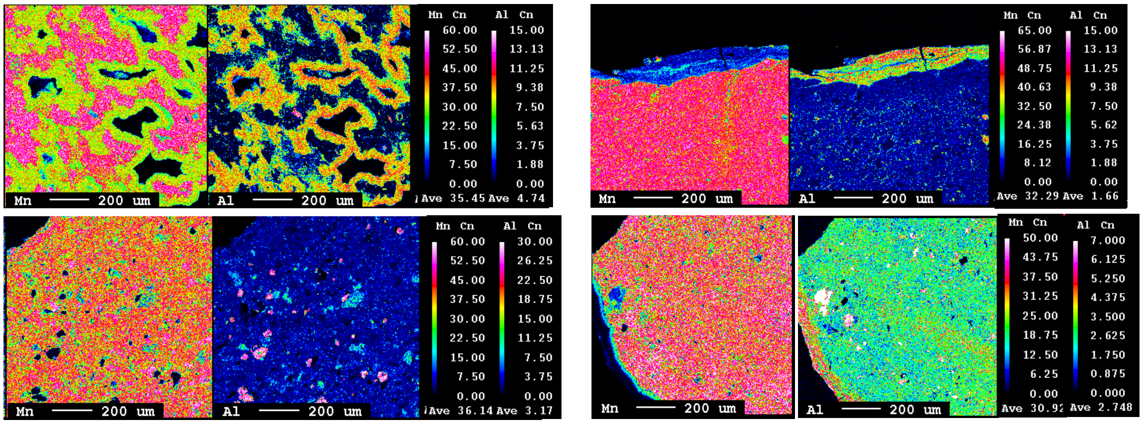

Picture 22: x-ray of manganese ore heated with argon, showing manganese and aluminum. From left, 500°C (A1), 700°C (A2), 1000°C (A3) and 1080°C (A5).

5.2 Reduction of Mn ore in methane

6 samples were purged with methane for one hour after they were heated in argon. The intention was to deposit carbon on the ore and to find the temperature where the deposition was most effective. An overview of the experiments is displayed in table 23.

Table 23: Overview of samples purged with methane.

Material	Sample #	Temperature [ºC]	Purging gas	Holding time	Mass [g] before	Mass [g] after	Reduction %
COMILOG ore	C1	700	CH_4	1 hour	200	166	17 %
COMILOG ore	C2	850	CH_4	1 hour	1000	762	23.8 %
COMILOG ore	C3	950	CH_4	1 hour	1000	795	20.5 %
COMILOG ore	C4	~900	CH_4	1 hour	1000	784	21.6 %
COMILOG ore	C5	1020	CH_4	1 hour	1000	803	19.7 %
COMILOG ore	C6	1070	CH_4	1 hour	1000	797	20.3 %

The development of temperature in the crucible is plotted in diagram 13. Samples C1, C2 and C3 had a distinct rise in temperature after the initiation of methane purging. Humidity was observed in the gas ascending from the crucible a short period after the purging was commenced, while the temperature rose. Moisture in the off-gas argue that the water-gas shift reaction has taken place.

C5 did not experience a spike in temperature, but had been heated prior to the experiment, in another experiment that had to be canceled. C6 experienced a decreasing temperature when the purging was commenced, arguing that endothermic reactions requiring energy from its surroundings took place.

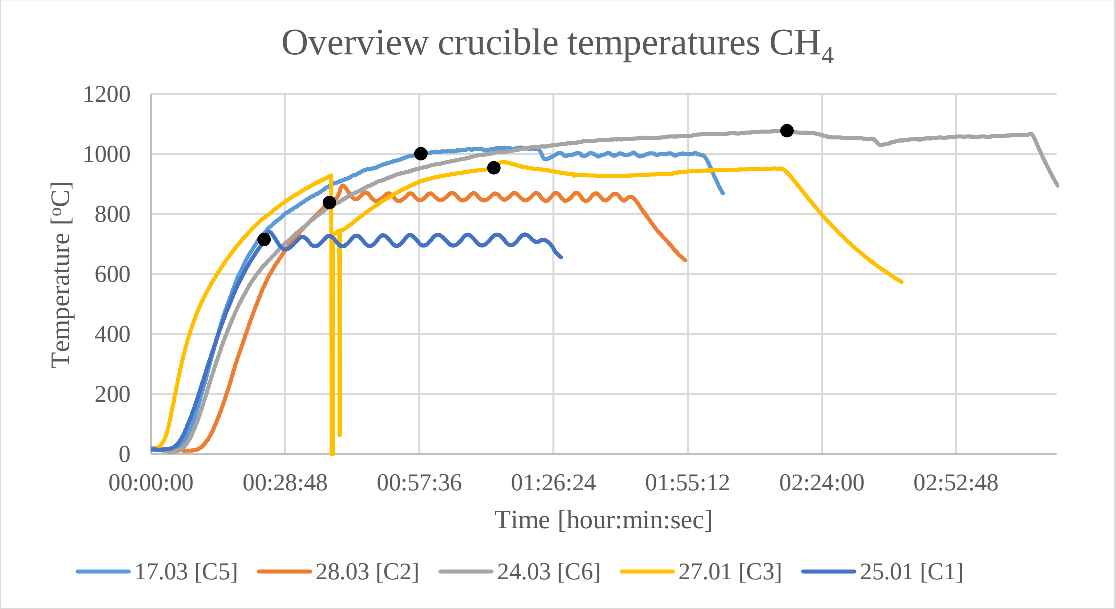

Diagram 13: Samples purged with methane. Black dot indicates the beginning of purging for the different samples.

As with the samples only heated in argon, the evacuation of oxygen is linked directly to the loss of mass, i.e. loss of mass is caused by the elimination of oxygen, and it is assumed that all the oxygen is leaving from a MnO_2 compound. The conversion caused by methane is calculated by using the values derived from the trendline calculated for the samples heated in argon. The total conversion is then divided between what is caused by the methane gas and what is caused by heat [32]. The conversion caused by methane can be seen in diagram 14.

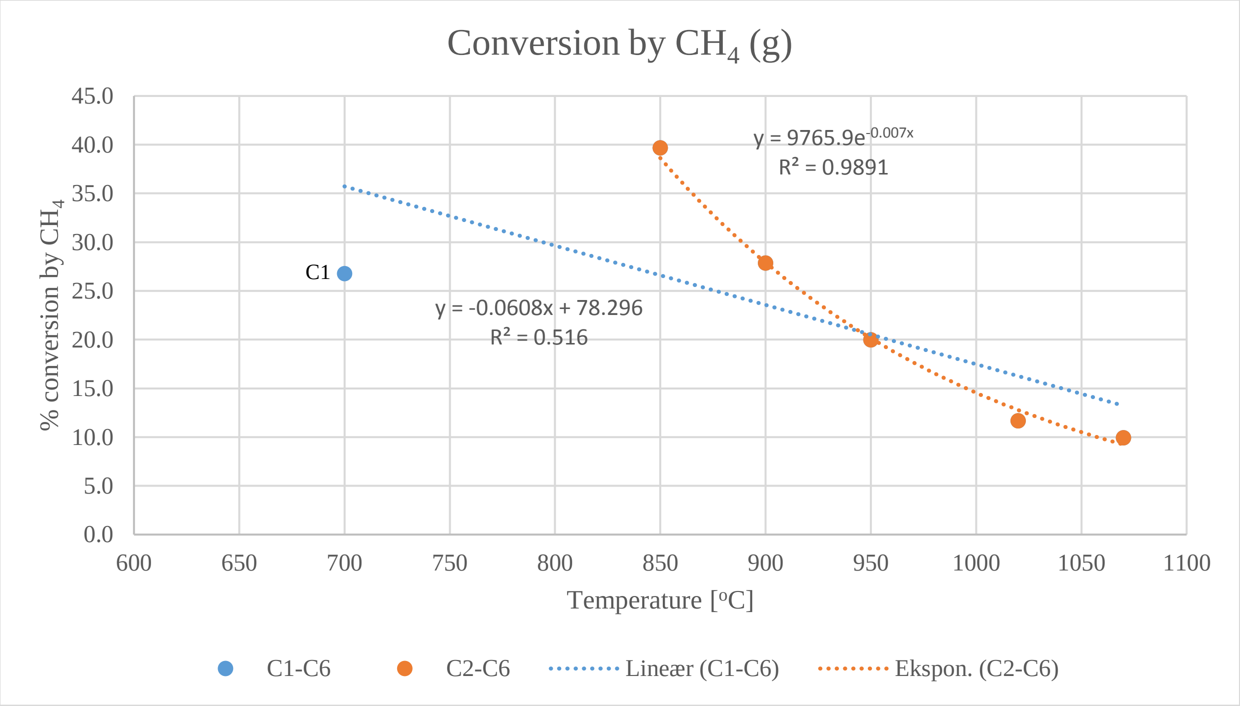

Diagram 14: MnO_2 conversion done by methane.

From the trendlines plotted, we assume that point C1 is an abnormality, and thus only looking at samples C2-C6, the Expon trendline, where the R value is close to 1. The trend line decreases exponentially, and the conversion effect of methane decreases with increasing temperature.

Carbon was deposited on sample C3 and C6. For C6, it was not possible to observe the layer in the x-ray analyze, but in sample C3, the outermost layer had a carbon content of 30 wt%, possibly being the layer of deposited carbon. The deposition was much smaller for both samples than what was expected compared to the result from the report done in TMT4500.

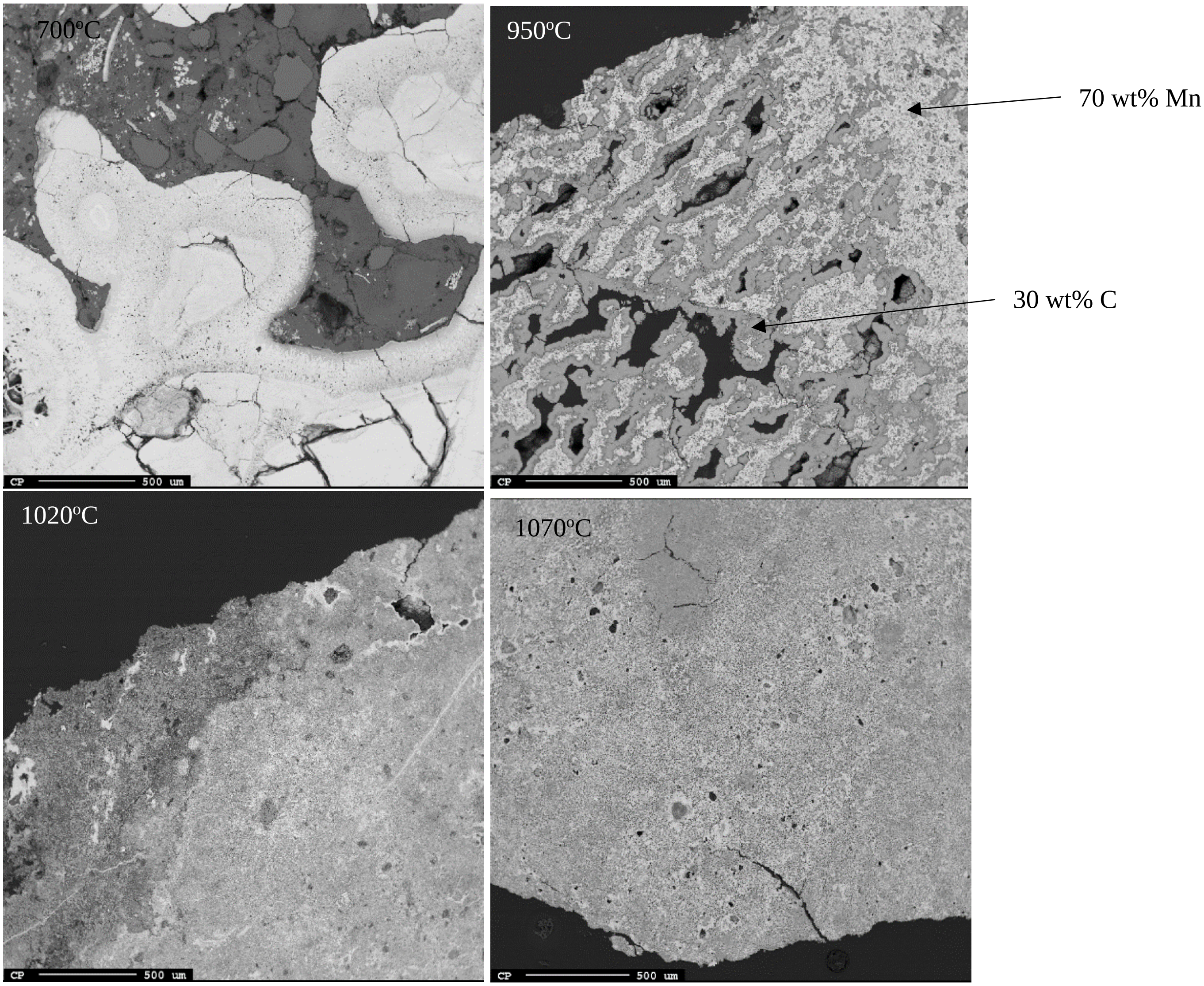

Picture 23: From left – manganese ore heated to 700ºC (C1), 950ºC (C3), 1020ºC (C5), and 1070ºC (C6) purged with methane for one hour.

The white, manganese rich grain in sample C1 has a layered structure with alternating amounts of oxygen. This particle was heated to 700ºC, and had a mass reduction of 17 wt%.

C2, heated only to 850ºC, had the largest reduction of mass. This can possibly be caused by the Boudouard reaction being more effective at this temperature compared to other temperatures that was tested, producing more CO gas to reduce the higher manganese oxides.

The x-ray of sample C3, heated to 950ºC, showed an approximate carbon concentration of 30 wt% around the surface and pores, possibly being the deposited carbon. The concentration of oxygen is higher closer to the surface and around pores.

C5 has a layered structure could indicate that the particle has reduced in agreement with the unreacted shrinking core model. The area is not continuous around the entire particle, shown in picture 24, lower left. This is presumably caused by the unreacted parts not being exposed to methane at the same degree.

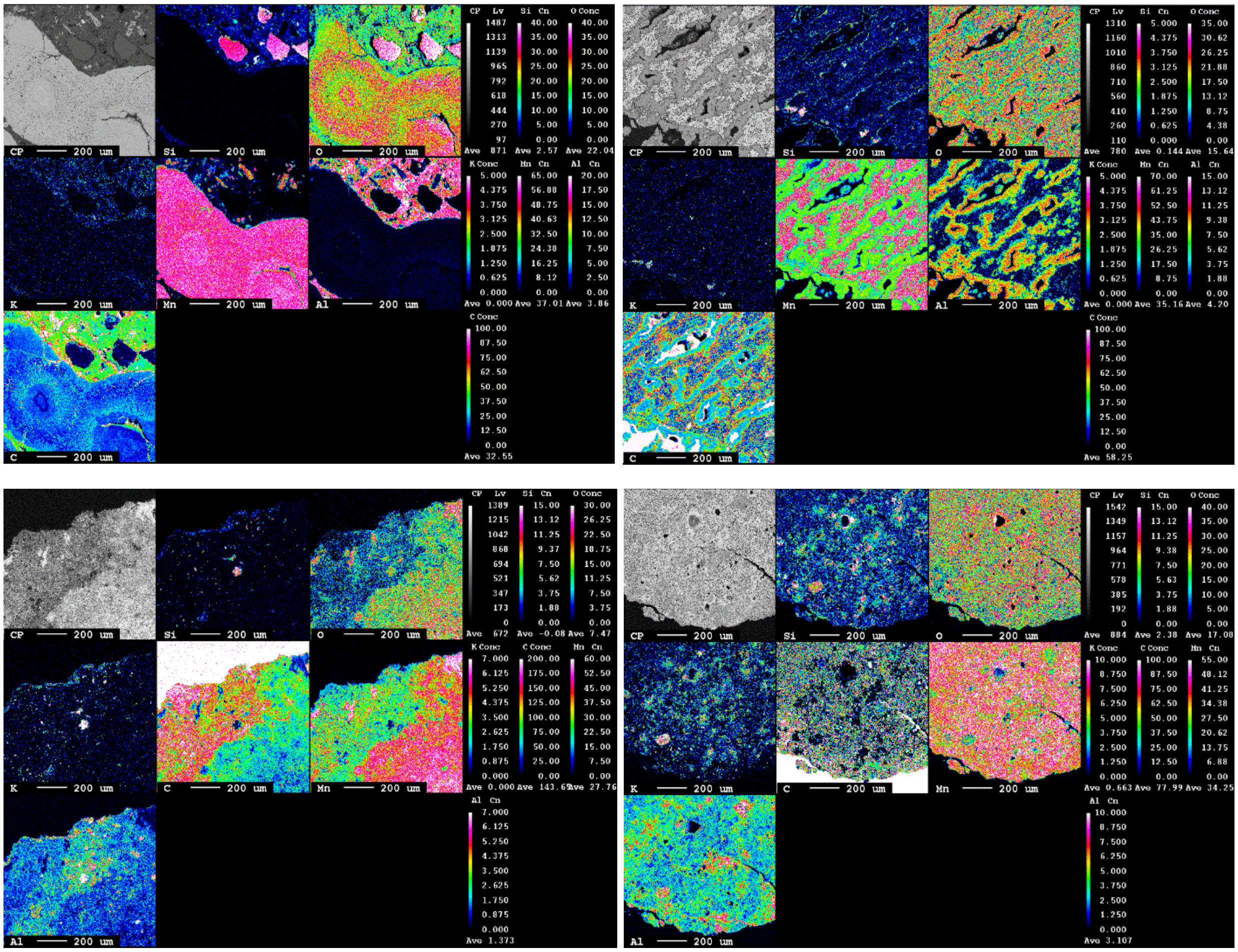

Picture 24: x-ray analysis of ore reduced with natural gas. From top left, C1 (700°C), C3 (950°C), C5 (1020°C) and C6 (1070°C)

Sample C6 was the only sample that experienced a decrease in temperature after the purging of methane was commenced. This suggests that endothermic reactions requiring energy have taken place in the crucible when methane was purged through the ore. It also had a very even matrix composition. In the x-ray analysis, it can be noted that the concentration of oxygen is lower closer to the surface of the particle than in the center of the particle, shown in picture 24, complying with the unreacted shrinking core model.

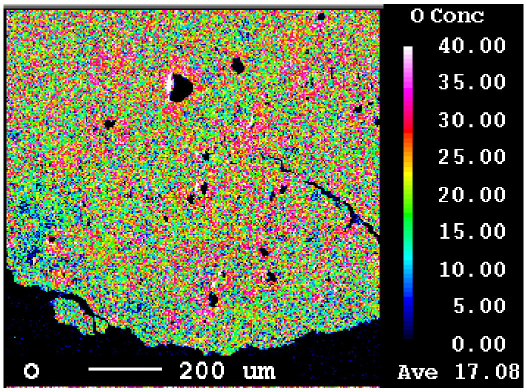

Picture 25: Sample C6, purged in methane at 1070°C

Sample C6 is in line with the shrinking unreacted pore model as it has a decreased concentration of oxygen close to the surface of the article compared to the rest of the matrix. This sample was also the only one experiencing a temperature reduction after purging was commenced, instead of an increase. This suggests that endothermic reactions that require energy have taken place in the crucible after the methane was in contact with the oxides.

5.3 Deposition of carbon

Table 24: Overview of samples with deposition of carbon.

Sample	**Deposited carbon**
C1	no
C2	no
C3	yes
C4	no
C5	no
C6	yes

Results from the report written in TMT4500 [10] proved it possible to deposit carbon from natural gas onto the surface of manganese ore. Picture 25 reveal a layered structure on the ore surface. The picture to the right, where the concentration of manganese is analyzed reveals an outermost layer that is not shown on the picture on the left, where carbon concentration is analyzed. This is likely the layer of deposited carbon.

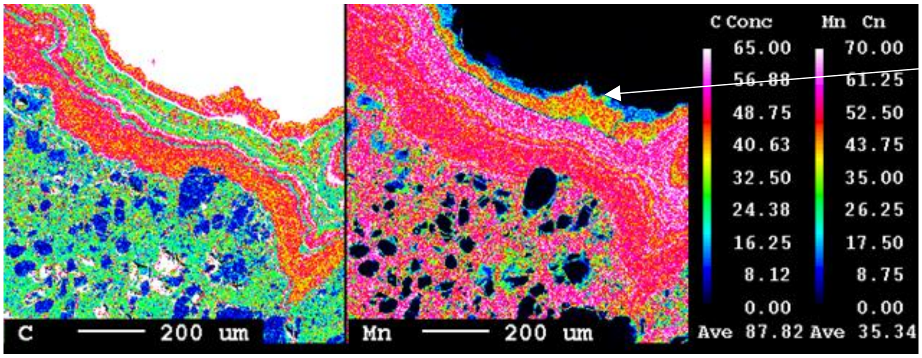

Deposited carbon layer

Picture 26: X-ray of manganese ore with visually observed deposited porous carbon layer, sample F6 heated to 1000ºC.

Similar results were found in sample C3 and C6, but a smaller amount of carbon was deposited on the ore. X-ray analysis of sample C6 did not show deposited carbon. Sample C3, depicted in picture 26, has a layer around the pores and surface with 30 wt% C. Compared to the similar structure found in sample A1 being, manganese ore heated to 500ºC, no accumulation of carbon in the second phase was observed. A1 is shown in picture 27 for comparison.

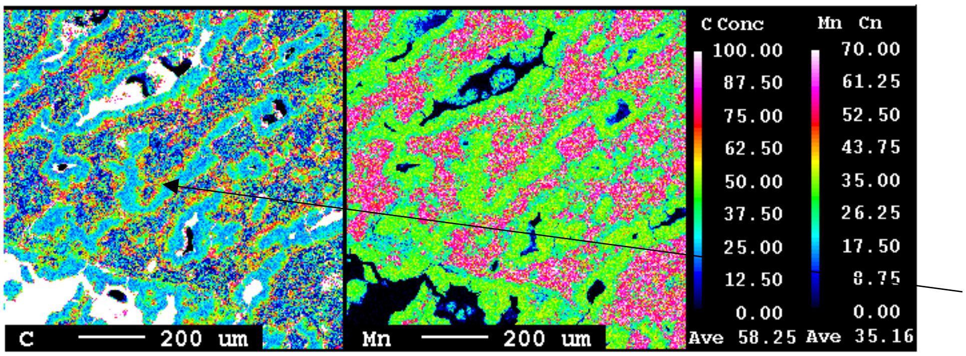

Possibly the carbon deposition.

Picture 27: Sample C3, heated to 950ºC

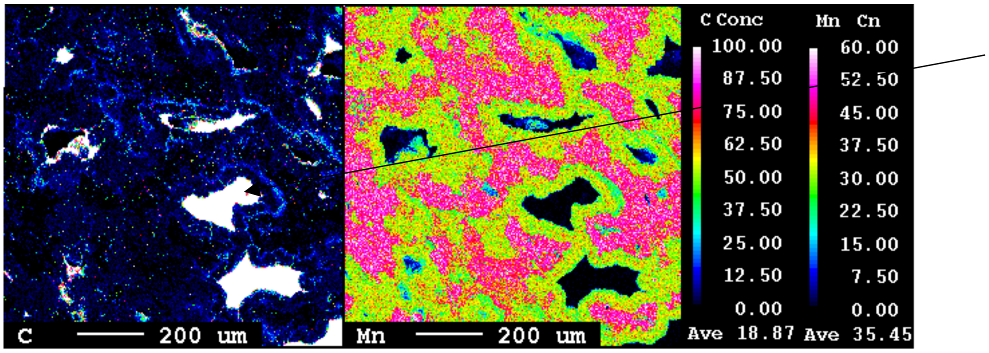

Pores filled with epoxy, but no accumulation of carbon on the edges

Picture 28: Sample A1, heated to 700ºC for comparison.

X-ray analysis of sample C5 also showed a surface layer that could possibly be deposited carbon, as it had a high carbon content, but it was hard to tell by visual inspection. This layer was not continuous around the particle, and the x-ray was taken at the transition point. The samples were covered with carbon before they were studied in the electron probe microscope, which can be one of the reasons that the highest amount of carbon registered is 200 wt %.

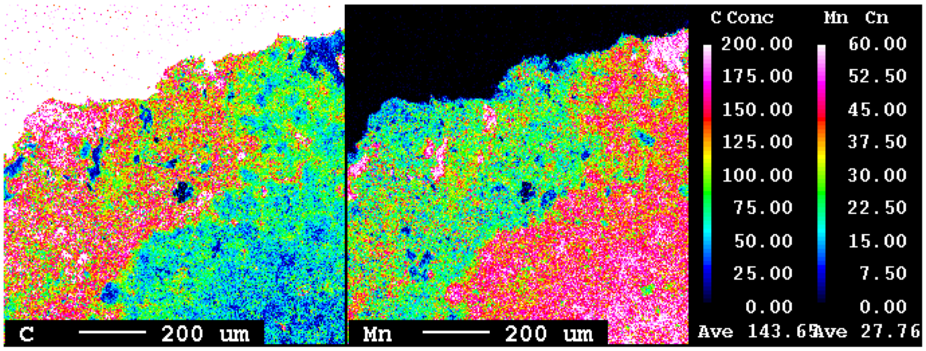

Picture 29: Sample C5, possible deposition of carbon.

Less carbon than expected was deposited on the ore during this project. The x-ray pictures show different vastly different results. In table 24, parameters between experiments done in TMT4500 and now are compared to look at possible causes of the reduced deposition.

Table 25: Comparison of parameters fall and spring.

TMT4500, F6, heated to 1000ºC	**Now**
fresh ore	Same ore, but stored for 8 months
5.0 CH_4	5.0 CH_4
Temperature ~1000ºC	Temperature ~1000ºC
Ramping time 40ºC/min	Ramping time 35ºC/min
	Trouble with thermoelement, was repaired
Crucible used for other projects as well	
Sulphur?	Sulphur?

Xue E. et al [33] found that sulphur compounds can cause deactivation of the catalysts that catalyze the water gas shift reaction. Under these conditions, sulphur is most likely be in the form of H_2S (g).

Pretreatment of the ore or storage may have caused contamination of the ore, affecting the content of sulphur when it was crushed to achieve the correct size.

The ore has been stored in a plastic container, and the samples taken then where lying on the top. The amount of ore has decreased, and now, the ore has been taken from the bottom of the original container.

Other people have been using the furnace and crucible, perhaps leaving residue on the inside of the crucible, which may have catalyzed the cracking of methane.

5.4 Contemporary deposition and reduction

Project in TMT4500 [10] found that a porous carbon layer was deposited onto the manganese ore when it was purged with methane for one hour at 1000ºC. Furthermore, the deposition of the carbon only begun after the initial reduction of the higher manganese oxides.

Diagram 14 show the conversion of MnO_2 by methane as a function of time. For all experiments except C6, an increase in temperature accompanied by humid gases ascending from the crucible argue that a reduction has taken place. C3 and C6 was the only experiments were carbon was deposited, but had different response to the methane – the temperature increased for C3, while it decreased for C6. The reduction of the higher manganese oxides are exothermic reactions, releasing energy, indicating that a reduction has happened. A decrease in temperature, however, indicates that endothermic reactions have taken place – cracking alone is an endothermic reaction that requires energy. Due to the small amount of carbon deposited, it is likely that the Boudouard reaction has taken place as well, producing CO gas from solid carbon. This direction of the Boudouard reaction is endothermic.

C6 was conducted at the highest temperature, and it is thus possible that there is a shift in the reaction rates when the temperature reaches this point, altering the equilibrium of the reactions.

5.5 Reduction mechanisms

The only parameter varied in the experiments was the temperature, while gas concentration and purging time was held constant for all experiments where methane was used. The ore heated in argon had different ramping times, and the length of time the ore was exposed for heat varied accordingly.

Reduction in the form of oxygen removal is assumed here. Several different structures were found in the ore, making it hard to compare the samples and identify how the reduction had proceeded. The same structure was found in sample A1, heated to 500ºC in argon, and C3, heated to 950ºC and purged with methane, making the two of them easier to compare. Two samples of C3 were analyzed in the electron microprobe, displaying two different structures within the same sample. The amount of oxygen in both is seen in picture 30.

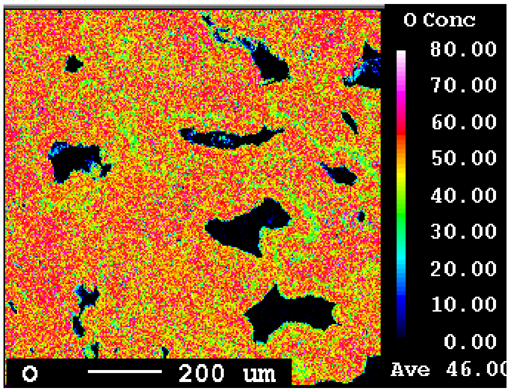

Picture 30: Oxygen concentration in sample A1, manganese ore heated to 500ºC in argon.

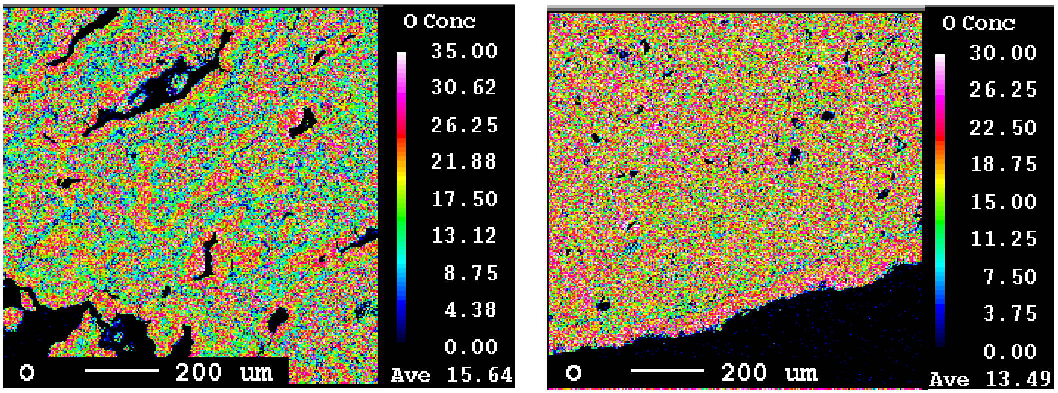

Picture 31: Oxygen concentration in the two C3 samples, heated to 950ºC and purged with methane.

A1 has an oxygen concentration close to 60 wt%, whereas it in C3 is closer to 20 wt% at the surface and around pores. C3 was heated to a higher temperature, and held there plenty longer A1. The C3 sample to the left has a higher concentration of oxygen close to the surface and around pores, contradicting the unreacted core model, were the highest oxygen concentration would remain in the core of the particle if the reduction acted accordingly. The sample to the right has an even distribution of oxygen around 20 wt%, and it is thus difficult to say how the reduction have advanced in the sample.

Evidence of the water-gas shift reaction was observed for 4 of the samples, heated to 700^{o}C, 850^{0}C, 900^{o}C and 950^{o}C, when methane first came in contact with the ore. Combined with a spike in the temperature, there is evidence that the overall reaction is exothermic. Sample C6, heated to 1070^{o}C, was the only sample where the temperature decreased after the purging of methane was commenced, indicating that the overall reaction is endothermic. Carbon was deposited on sample C6, but as the amount was smaller than what would have been expected from the results in the TMT4500 project, it is a possibility that the reversed Boudouard reaction have taken place, where solid carbon and CO_2 are converted to CO gas.

The different observations in C3 and C6 suggest that more than one deposition mechanism can take place, depending on the temperature it has been exposed for.

5.6 Discrepancies and evaluation of method

The deposition of carbon was verified visually, which was difficult to determine for some samples. No equipment was available to detect the composition of the gases ascending from the crucible, making it hard to tell what reactions may have taken place during heating and the purging of methane. The oxygen values from the mass analysis was to large compared to the amount of manganese, and the mass analysis done in different spots is not always reliable. The mass percent of oxygen was thusly disregarded, and other calculations were made. Consequently, the results are reasonably trustworthy, but there are errors regarding element concentrations especially, and hard to say anything certain about reactions that have taken place in the crucible.

The furnace struggled in some of the experiments to achieve the wanted temperature and keeping it stable. This caused several experiments to be executed at temperatures lower than planned. A defect with the thermocouple was suspected, and the wires connecting it to the furnace was changed, and the thermocouple end was cut off and welded anew.

The samples were left to cool in the crucible overnight, with no flow of argon gas. As manganese carbide easily decompose in air, it’s possible that manganese carbide has been formed, but decrepitated before the ore was removed from the crucible for examination.

Orientation of the particle during polishing can be partly responsible for the appearance of the particle in the microscope.

6 Conclusion

- Carbon from methane was deposited on manganese ore, but less than what was expected from earlier results.
- Observations indicate that two different reduction mechanisms have taken place.
- Calculations indicate that the conversion effect of MnO_2 by methane decreases with increasing temperature, and that most of the reduction was non-isothermal, caused by heat.
- Aluminum seem to diffuse towards the particle surface while it is heated and still in a solid state.
- Some of the observations indicate that the ore reduce as stated in the shrinking unreacted core model.
- The subject needs further investigation to figure out the mechanism causing carbon to be deposited, why deposition varies and the mechanisms of reduction.

7 References

1. Olsen SE, Tangstad M, Lindstad T. Production of manganese ferroalloys. Trondheim: Tapir akademisk forl.; 2007.
2. Kofstad PKP, Bjørn. Mangan https://snl.no/mangan: Store Norske Leksikon; 2017 [updated 27. august 2016; cited 21. february 2017].
3. Takamichi Iida RILG. The thermophysical properties of metallic liquids. Oxford: Oxford University press; 2015. 353 p.
4. https://en.wikipedia.org/wiki/Manganese#/media/File:Mangan_1-crop.jpg. [updated 6 December 2016].
5. Tangstad M. Metal production in Norway. Oslo: Akademika Publ.; 2013.
6. Haque ND, Mailsja. Greenhouse gas emission assessment of bio-coke from wood for application as bioanode in aluminum production. Faculty of Engineering and Industrial sciences, Swinburne University of Technology. 2012.
7. Demirbas A. Methane Gas Hydrate. Dordrecht: Springer; 2010.
8. Rosenqvist T. Principles of extractive metallurgy. 2nd ed. ed. Trondheim: Tapir Academic Press; 2004.
9. Dalaker H. Methane and natural gas as a reducing agent. SINTEF, 2011 SINTEF A 19858.
10. Svoen S. Carbon deposition from natural gas onto manganese ore. NTNU, 2016.
11. Abbas HF, Wan Daud WMA. Hydrogen production by methane decomposition: A review. International Journal of Hydrogen Energy. 2010;35(3):1160-90.
12. Zhang T, Amiridis MD. Hydrogen production via the direct cracking of methane over silica-supported nickel catalysts. Applied Catalysis A: General. 1998;167(2):161-72.
13. Rahman M, Croiset E, Hudgins R. Catalytic Decomposition of Methane for Hydrogen Production. Topics in Catalysis. 2006;37(2):137-45.
14. Ostrovski O, Zhang G. Reduction and carburization of metal oxides by methane-containing gas. AIChE Journal. 2006;52(1):300-10.
15. Dalaker H, Tetlie P. Decomposition of methane during oxide reduction with natural gas. 2014. p. 537-46.
16. Alizadeh R, Jamshidi E, Zhang GP. Transformation of methane to synthesis gas over metal oxides without using catalyst. J Nat Gas Chem2009. p. 124-30.
17. Anacleto N, Ostrovski O, Ganguly O. Reduction of manganese oxides by methane-containing gas. ISIJ International. 2004;44(9):1480-7.
18. Ostrovski O. The use of natural gas for reduction of metal oxides: Constraints and prospects. 2014. p. 529-36.
19. Sorensen B, Gaal S, Ringdalen E, Tangstad M, Kononov R, Ostrovski O. Phase compositions of manganese ores and their change in the process of calcination. International Journal of Mineral Processing. 2010;94(3-4):101-10.
20. Boudouard reaction.
21. Tangstad M. Mn-seminar. 2016.
22. Aderibigbe DAS, J. . Studies in coke reactivity. Part 1. Reaction of conventionally produced coke with CO-CO_2 mixtures over temperature range 850°-1000°C. Ironmaking and steelmaking 1. 1981:11-9.
23. Newsome DS. The Water-Gas Shift Reaction. Catalysis Reviews. 1980;21(2):275-318.
24. Lobo S. Reduction of manganese ores using CO, H_2, CO_2 and H_2O blends. Trondheim NTNU, 2015.
25. M. Bahgat KSAH, H.A. El-Kelesh, M.I. Nasr. Fundamental Study of Water-Gas Shift Reaction in Ironmaking Process. Journal of metallurgical Engineering. 2012;1(3):63-9.
26. Kolbeinsen L. In: Svoen S, editor. 26.05.2017.
27. Berg KL. Gaseous reduction of manganese ores. Trondheim: Department of Metallurgy, Norwegian University of Science and Technology; 1998.

28. Seetharaman S, Institute of Materials M, Mining. Fundamentals of metallurgy. Cambridge: Woodhead Publ. and Maney Publ. on behalf of the Institute of Materials, Minerals & Mining; 2005.
29. Weinberg MC, Birnie DP, Shneidman VA. Crystallization kinetics and the JMAK equation. Journal of Non-Crystalline Solids. 1997;219:89-99.
30. Type S thermocouple 2011. Available from: http://www.thermocoupleinfo.com/type-s-thermocouple.htm.
31. Eom C, Min D. Kinetics of the formation reaction of manganese carbide under various gases. Metals and Materials International. 2016;22(1):129-35.
32. Kolbeinsen L. 2017.
33. Xue E, O'Keeffe M, Ross JRH. Water-gas shift conversion using a feed with a low steam to carbon monoxide ratio and containing sulphur. Catalysis Today. 1996;30(1):107-18.